RHEOLOGICAL CHARACTERIZATION OF MINERALS

A
Thesis

submitted in partial fulfillment of the requirements for the award of degree of

Master of Engineering (M.E.)

In
Thermal Engineering

Submitted by
NITIN KUMAWAT
(ROLL NO. 801383018)

UNDER THE GUIDANCE OF

Dr. SATISH KUMAR
Assistant Professor, MED
Thapar University, Patiala

Dr. S.K MOHAPATRA
Senior Professor and HMED
Thapar University, Patiala

DEPARTMENT OF MECHANICAL ENGINEERING
THAPAR UNIVERSITY, PATIALA – 147004
JULY 2015

CERTIFICATION

I, Nitin Kumawat, declare that this thesis report entitled "***Rheological characterization of Minerals***", submitted towards fulfillment of the requirements for the award of Master's Degree in Thermal Engineering, in Mechanical Engineering Department of Thapar University, Patiala, is entirely my own work. This document has not been submitted for any degree in any other institution.

Date: 15/7/2015
Place: Patiala

Nitin Kumawat

Nitin Kumawat
801383018
Thapar University, Patiala

This is to certify that above statement made by the candidate is correct and true to the best of my knowledge.

Dr. Satish Kumar
Assiatan Professor,MED
Thapar University, Patiala

Dr. S.K Mohaparta
Senior Professor and HMED
Thapar University, Patiala

Countersigned by

Dr. S.K. Mohapatra
Sr. Professor and Head
Mechanical Engineering Department
Thapar University, Patiala

Dr. S.S. Bhatia
Dean
Academic Affairs
Thapar University, Patiala

ACKNOWLEDGEMENT

I would like to express my deepest gratitude to my supervisor, Dr. S.K Mohapatra, for his excellent guidance, caring, patience, and providing me with an excellent atmosphere for doing research. Your advice on both research as well as on my career have been priceless. The opportunity, support, exposure and atmosphere provided by the Thapar University, Patiala, to carry out my studies are highly appreciated.

I also express my special thanks to Dr. Satish Kumar, Assistant Professor and PG. coordinator, providing me opportunity to conduct this work and bring it out in present from.

A special debt of gratitude is owed to the authors whose works I have consulted and quoted in this work. Last but not least, I am forever grateful to my parents, family and friends for their unconditional support and best wishes.

Nitin Kumawat

Nitin Kumawat

ABSTRACT

In the present study rheological behaviour and characterization of minerals are investigated by using Anton Paar RheolabQC rheometer to generate extensive rheological data. Four types of minerals viz. iron ore (hematite), zinc ore, iron ore (magnetite) and lime were taken for investigation. The particle size distribution, pH, Scanning Electron Microscopy (SEM) analysis, Energy Dispersive Spectroscopy (EDS) etc. was studied using various bench scale test with standard procedure. The rheology of mineral suspension with the variation of solids concentration, temperature, and fraction of coarse particles are performed. The rheological data shows that upto 30% solid concentration, mineral suspension shows Newtonian behaviour and beyond this shows non-Newtonian behaviour. The rheological investigation of the finner particulate of mineral suspension of iron ore (hematite) and zinc ore slurry is also carried out with the addition of coarser particulate. It is observed that viscosity of both mineral suspension are improved. The temperature effect on the rheological properties of mineral suspension also studied. The rheological data obtained was used to evaluate the pressure drop of mineral ore slurry flowing through straight pipe. It is found that for mineral slurry flowing through pipeline the pressure drop increases with increase in velocity and solid concentration.

TABLE OF CONTENTS

LIST OF FIGURES

LIST OF TABLES

NOTATIONS

τ	: Shear stress (Pa)
μ	: Dynamic viscosity
$\frac{dv}{dy}$	: shear rate, rate of strain or velocity gradient
Re	: Reynolds number
ρ	: Density (kg/m^3)
V	: Mean flow velocity (m/sec)
D	: Pipe diameter (mm)
τ_y	: Yield stress (Pa)
C_w	: Weight concentration of slurry (wt. %)
d_{50}	: Mass median particle diameter (microns)
K	: Flow consistency coefficient
g	: Acceleration due to gravity (m/s^2)
γ	: Shear rate (1/s)
η	: Apparent viscosity (Pa-s)
ω	: Angular frequency (Hz)
x	: Optical path difference
ρ_m	: density of slurry (lb/ft^3, kg/m^3)
ρ_s	: density of the solids (lb/ft^3, kg/m^3)
ρ_l	: density of liquid without solids (lb/ft^3, kg/m^3)

CHAPTER 1

INTRODUCTION

1.1 BACKGROUND

Since the ancient time of civilization, mining industry plays important role in developing the social, economic and industrial development. Due to the rapid growth in population, importance of mining industry increases suddenly over the last century. Technological advancements is also a main reason for its popularity. Nowadays mining industries contribute in many fields including agriculture, transportation, construction, energy, health etc. With the increase in the demand of minerals depletion in high grade mineral observed. This made the industries to develop finely disseminated low grade ore bodies.

Mineral ore body may contain about 1%-2% valuable minerals or even less. For extremely valuable minerals like gold, only a few grams/tonne may be efficient usable. This indicates that a lot of gangue material will also be taken out during mining process. Slurry form is used for the transportation and processing of mineral ore. Water is used for the production of slurry because of its easily availability and cheapness. Mining operation rate is greatly influenced by processing rate, rheological properties of the slurries and the solids concentration. In recent years focus is being placed on improving the design and optimization of mineral-processing operations to reduce costs. For achieving this, actual properties of the slurries being processed including the rheological properties that can be determined to represent the realistic condition found in actual site operations.

By 1374, zinc was found in metallic form in India. From 12^{th} to 16th century zinc metal was used for making brass and zinc oxide are used in medical purposes. Generally zinc ore is a mixture of coper, silver, gold, lead and other metals. Usually zinc ore contains 3% to 15% zinc. Iron ore is primary raw material for the production of steel. Australia, Brazil, India, South Africa and China are the largest producers of the iron ore. Iron ore are rich in iron oxides, it is found in the form of hematite (Fe_2O_3), magnetite (Fe_3O_4), limonite ($FeO(OH).n(H_2O)$), goethite FeO(OH), siderite ($FeCO_3$). Ore containing higher percentage of hematite and magnetite called natural ore and it

can be fed into blast furnace directly. Lime is an inorganic material containing carbonates, oxides and hydroxides of calcium. It is generally used for building material. Lime is classified as pure, poor and hydraulic lime also identify by its magnesium contents.

Mineral mixture can be divided into two broad categories: settling slurries and Suspensions slurry (non settling/slow settling slurries). Suspensions slurry contains fine particles at high concentration. Fine particles settled with slow rate which means that rheological properties can be measured using generic standard rheological instruments. Settling slurry consists of heavy particles, so they settle with faster rate which means that rheological properties of these slurries can be measured in standard instruments including: capillary tube, parallel plate, bob and cup.

1.2 MINERAL UTILIZATION

Zinc ores, Lime and Iron ore are found in just a relatively few areas, they are unevenly distributed in the earth's crust. It takes an exceptional arrangement of circumstances to make them, so it is very difficult to recognize the signs of a mineral deposit. Proper knowledge and experience requires for locating these mineral deposits. Geologists may take several years for locating a valuable mineral deposit. Several factors determine whether mineral deposit be profitably or not, it depends on mineral content, deposit size, processing costs, extracting efficiency and market value of minerals.

Iron ore is generally refined to create pig iron (metallic iron), which is utilized to make steel. Iron is one of the most critical metals utilized as a part of developed and developing economies. There is additionally cast iron, wrought iron and layered iron auxiliary sheeting, a conspicuous material in the building development. The purest form of iron is firmly magnetic which melts around 1528° C. Magnetite mineral is utilized to evacuate impurities present in coal and its magnetic abilities empower it to reuse again. Ukraine, Russia and Brazil are the largest producer of iron ore. Australia, USA, China, South Africa, India also contributed in iron production

Some mechanical procedures include the utilization of iron metal as a catalyst for chemical reactions, and it is likewise utilized as a part of procedures like photographic creating. It might be incorporated as a segment in abrasives and specially paints, similar to those utilized on outside structures that should be greatly weather

resistant Magnets, magnetic powders, and related items represent a few uses for iron mineral, as do some modern parts and auto parts.

After iron, aluminium, and copper, zinc is the fourth most generally consumed metal in the world. It has strong anticorrosive nature and links well with diverse metals. Thus, around one-half of the zinc that is created is utilized as a part of zinc galvanizing, which is the procedure of adding layers of zinc to iron or steel to anticipate rusting.

Another utilization of zinc is as alloy, the zinc is consolidated with copper and with different metals to shape materials that are utilized as a part of automobile, electrical parts, and household apparatuses. A third major utilization of zinc is in the generation of zinc oxide, which is utilized as a part of elastic assembling and as a protective skin ointment.

Lime is an essential compound that is utilized as a part of numerous modern procedures. It is used as a part of creation procedures to make steel, non-ferrous minerals, paper, plastics, fiber glass and building materials. Limestone and quicklime are key crude materials utilized as a part of iron and steel making procedures and are widely used for metallurgy draining, purifying and refining procedures to create non-ferrous minerals, for example, gold, copper, alumina, zinc, nickel, uranium, uncommon earth. Additionally used as a part of building materials, for example, concrete, mortar, steel, glass etc.

1.3 FLUID

Fluid is a continuous, amorphous substance whose molecule moves freely over another molecule and deform continuously under an applied shear stress and can take the shape of its container It include phases like liquid, gases, plasma and somewhat of plastic solids. Fluid has no shape and able to flow easily. For a fluid, shear stress is a function of strain rate. Pascal’s law defines the part of pressure in characterizing a fluid's state. Fluids can be classified depending upon the connection between shear strain and the shear stress and its subsidiaries.

1.3.1 Newtonian Fluids

Fluids which obey the Newton's law of viscosity and viscosity is independent of velocity gradient are called Newtonian fluids. Figure 1.1 shows graphical representation of shear stress versus shear rate, plotted as a rheogram in which shear stress and rate vary linearly and viscosity remains constant.

$$\tau = \mu \frac{dv}{dy} \tag{1.1}$$

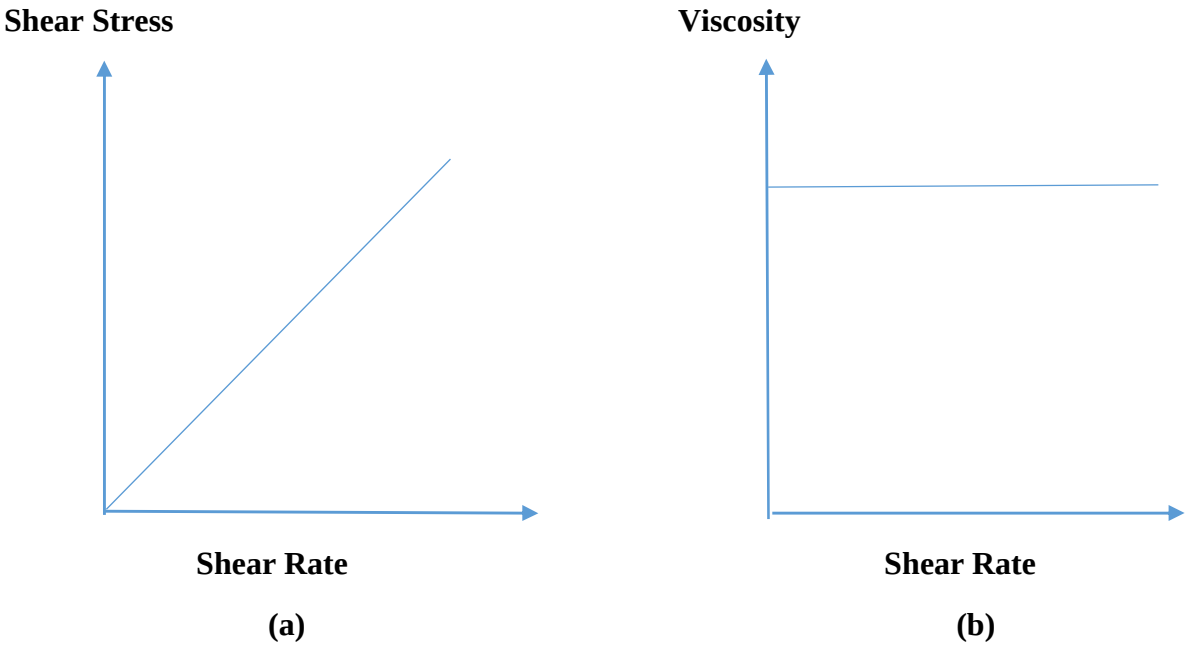

Figure 1.1: Rheogram flow of (a) shear stress vs shear rate (b) viscosity vs shear rate

1.3.2 Non-Newtonian Fluids

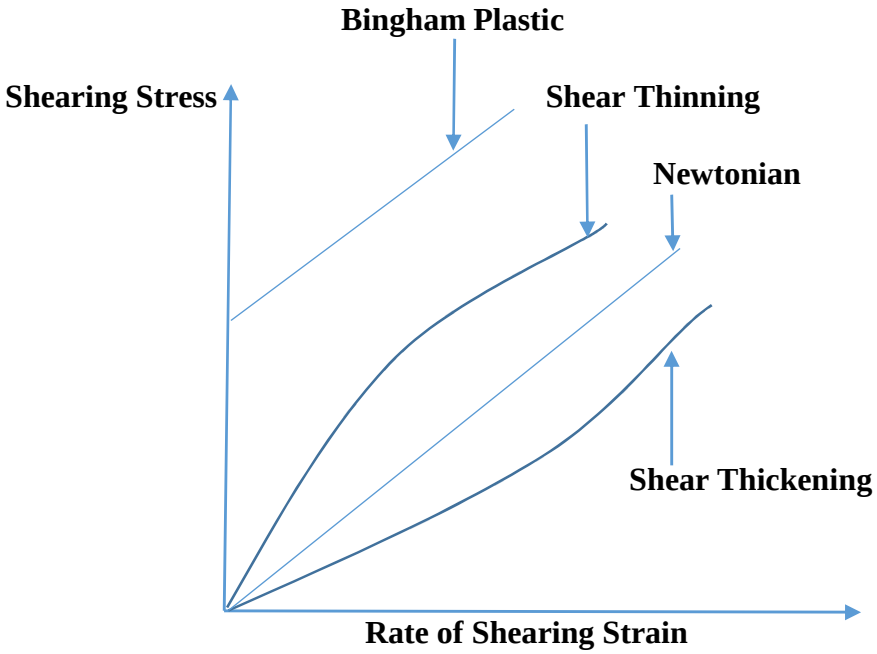

Figure 1.2: Rheogram of different fluid models

Figure 1.2 represents the Rheogram of different fluid models. The slope of the shear stress versus shear rate curve does not varies linearly, as shear rate changes. At the point when the viscosity reduces with expansion in shear rate. It is called shear- thinning fluid and in the reverse situation when the viscosity raises with the expansion of shear rate, the liquid is called shear-thickening. Shear-thinning fluid is more normal than shear-thickening. Shear- thinning liquids likewise called pseudo plastic liquids. Bingham plastics are an uncommon class of viscoelastic liquids that show a straight behaviour of shear stress against shear rate. Cases of viscoelastic liquids are mud, toothpaste, atomic fuel slurries and blood.

Fluid which don't comply with the Newton's law of viscosity is Non-Newtonian fluid and is comprehensively characterized as one for which the relationship shear stress/ shear rate is not a steady or when the shear rate is fluctuated, the shear stress doesn't change in the same extent. The resistance to flow arises because of the friction between layers. Ketchup, yogurt, blood, mud, gravy are the non-Newtonian fluids. The viscosity of these liquids changes with change in the shear rate. Parameters like velocity, shaft

and viscometer model all have impact on the consistency of a non- Newtonian liquid and this deliberate viscosity is known as apparent viscosity. Relation between the shear rate and the shear stress is time-dependent in non-Newtonian liquid. Viscosity changes with change in the stream condition.

A Bingham plastic is a viscoelastic material that acts as an inflexible body at low stresses but flows as a viscous liquid at high stresses. It is named after Eugene C. Bingham who proposed its numerical structure. It is utilized as a typical scientific model of mud stream in drilling designing, and in the treatment of slurries.

Shear thinning is a term utilized as a part of rheology to describe non-Newtonian fluids which have diminished viscosity when subjected to shear strain. The term is infrequently used to be an equivalent word for pseudo plastic behaviour, and is generally characterized as time-dependent effects, for example thixotropy.

1.3.3 Flow Regimes

There are three different types of Flow regimes viz laminar, turbulent and transitional flow. To calculate these flow regimes, Osborne Reynolds developed a relationship called Reynolds number which is directly proportional to the ratio between inertial and viscous forces.

$$Re = \frac{\rho V D}{\mu} \tag{1.2}$$

When Reynold number is less than 2000, flow is laminar and when Reynold number is greater than 4000, flow is turbulent. The region between both laminar and turbulent flow is unstable region called transition zone.

Reynold number for non-Newtonian fluid (Re)

$$Re = \frac{8\rho V^2}{\tau_y + K\left(\frac{8V}{D}\right)^n} \tag{1.3}$$

1.3.4 Laminar Flow

Figure 1.3 shows laminar flow of the fluid, It is a flow in which motion of the fluid particles is in orderly arrangement or fluid moves in a smooth way with all the particles moves parallel to the pipe in a straight line. It is often stated as streamline flow.

Pressure, velocity and other flow properties remains constant at each point. It is found in areas where flow channel is relatively small, viscosity is high and fluid moving slowly. Smoke rising from cigarette initially in a straight path is a laminar flow. After some time smoke changes to turbulent flow, as it swirls and eddies from its normal path.

1.3.5 Turbulent Flow

Turbulent flow is a flow in which motion of the fluid particles is in irregular shape, fluid does not moves smoothly and in straight line as shown in figure 1.4. Mixing takes place in comparison to laminar flow. In turbulent flow speed of the fluid changes continuously. Flow of river and wind are the example of turbulent flow.

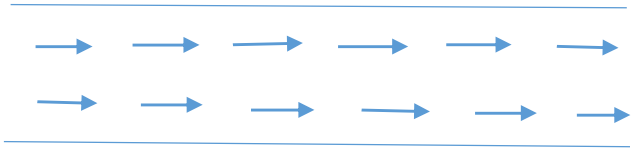

Figure 1.3: Laminar Flow

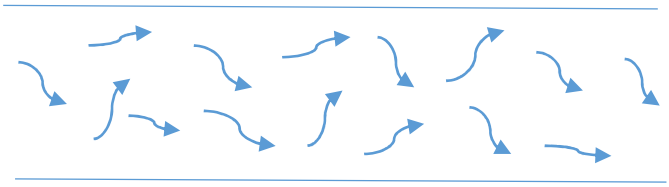

Figure 1.4: Turbulent Flow

1.3.6 Transitional Flow

Transitional flow is the region between laminar and turbulent flow region and is difficult to identify. It is known that turbulent flow occur above particular velocity and laminar flow occur below particular velocity. Therefore, transition region can be expressed as a region between these two velocities. Transition region is a function of Reynold number and velocity. Prediction of this region is very difficult due to unstable nature of this region.

1.4 VISCOSITY

Measure of the internal friction of a fluid is a viscosity and when a layer of fluid move relatively to another layer, friction becomes apparent. More is the friction more is the

amount required for the movement which is called shear. It determine strain rate of the fluid generated by applied shear stress. According to SI unit, viscosity is measured in Newton seconds per meter squared or Pascal second. It is thermodynamic variable varying as a function of temperature and pressure. Viscosity changes with change in the temperature but not greatly with pressure. In gasses, viscosity increases with increase in the temperature because of molecular interaction and in liquid, viscosity decreases with increase in the temperature because of increased spacing between molecules.

1.4.1 Rheology and Its Role in the Design of Transportation System

Rheology is used to describe fluid flow properties. It was founded by two scientists Professor Marcus Reiner and Professor Eugene Bingham 80 years ago. It is used to describe the viscosity and elasticity of the component. Viscosity shows resistance to flow or thickness and elasticity shows stickiness or structure. Rheology term originates from Greek word 'rheos' means 'the river', 'stream' and is defined ad science of deformation and flow of matter. Sir Isaac Newton proposed a direct relation between shear stress and shear rate which is valid for Newtonian fluid and not for non-Newtonian fluids. It is generally presented in a plot between shear stress versus shear rate, called rheogram. Rheology is the study basically in the fluid condition of matter, additionally as strong or delicate strong in which they react with plastic flow instead of disfiguring flexibly under applied force. It applies to substances such as sludge, polymers, glass formers, suspensions, mud, bodily fluids (e.g., blood).

For Newtonian fluids, viscosity changes w.r.t temperature but not with strain rate. Newtonian fluids defined by a single coefficient of viscosity for a particular temperature. But for non-Newtonian fluid viscosity changes with the strain rate. Rheology by and large records for the conduct of non-Newtonian liquids, by illustrating the minimum number of capacities that are obliged to co-relate stresses with change of strain rates. Viscosity of pseudo plastic fluid reduced by shaking because of relative movement of the layers but not happened in case of water. Increase in relative velocity reduces the viscosity of shear thinning material while in shear thickening material viscosity increases with relative deformation.

The Rheological properties of slurry suspensions are of great importance in various industrial applications including pipeline transportation of slurries. Relationship between pressure drop and flow rate can be calculated by rheological data. These parameters can also be used to calculate life of pipeline, wear rate and power required to mix the slurry in the tank. The rheological characteristics of a slurry suspension depends on various parameters like particle size distribution, shape, solids concentration, size, carrier fluid properties etc. By keeping the other parameters same and manipulating particle size stabilizes slurry suspension. The rheological data is required to obtain the head of the slurry pump and the presence of solid particles disturbs the operation of the pump.

Different particle material will have different properties like density, shape and size which affect the rheological properties, hence the flow pattern will differ from material to material in a slurry pipeline. Generally for commercial purposes slurry is non-Newtonian in concentration.

It is more difficult for us if the slurry behaves as non-Newtonian. It is essential to have proper knowledge and understanding of the rheological properties while introducing these parameters for commercial use. For predicting the parameters of non-Newtonian slurry, viscometric test should be avoided if particle shape and size is not known. For large particle sized slurry viscosity measurement is difficult because these particles settle down during measurement and affects the uniformity of the solution. To overcome this problem large particles should be removed and test carried out with fine particles.

1.5 MOTIVATION FOR THE PRESENT STUDY

The transportation of mineral slurries through pipeline is accomplished by planning slurry transportation components that advances economic transport with a minimum pressure drop. At low concentration, slurry behaves Newtonian and the flow in the pipelines keeps up a consistent consistency at the different shear rate. Likewise, in mineral slurry, highly concentrated slurry is needed in atomized structure that is subjected to high shear rates. These highly concentrated slurry normally show non-Newtonian flow behaviour with viscosities fluctuating with the rate of shear. Along these, before planning a slurry transportation framework, it is of principal significance to focus the rheological behaviour of mineral slurries to know the different parameters

like the viscosity at different concentrations, flow behaviour, the pressure drop etc. The present study was directed to create broad rheological information and focus the mineral slurry rheological behaviour that best describe the mineral specimens at different solid concentration, particle size distribution, and mineral fines.

CHAPTER 2

LITERATURE REVIEW

A lot of research work is carried out in the past on the rheology of slurry suspension by many researchers, which sets roots and base for advance work in this investigation. This acts as a guideline for this thesis and give better understanding of the topic. Factors that affects the rheology of minerals have been inspected by many researchers and an optimum value for slurry transportation with viscosity in a specific shear rate has been found. The main emphasis of the following study is on the mineral slurries and its applications in several areas. In this study, earlier to the research work, a widespread review of the published works in mineral rheology field with factors like particle shape, size, its properties, temperature, pH, chemical additives etc were taken. The rheology of minerals and their characterization has received attention in recent years because of widespread application in industry and academic interest.

Yavuz et al. (1998) studied the impact of particle size distribution on the Rheology of Lignite - Water slurry. The lignite sample was sieved into six different particle sizes: <45, 45 - 53, 53 - 63, 63 - 75, 75 - 90, 90 - 125 μm. Rheology experiment perform at 60% concentration by weight at 20°C. They found high viscosity value for fine particle which is not suitable for the flow of slurry suspension and with the addition of courser particle (90 - 125 μm) viscosity of slurry suspension improved.

Mishra et al. (2002) examined the rheological properties of coal water slurry produced by Indian coal. The influence of pH, ash contents, temperature and solid concentration on the rheology of coal water slurry was studied. The three samples of coal were obtain from Talcher coal field, Orissa, India having ash content 11.4%, 27.4% and 34.6%. Rheological investigations of the coal water slurry (CWS) was completed in a HAAKE rotational viscometer RV30 using sensor MV1 at 25°C. To maintain the temperature of slurry with accuracy of ±0.1°C a thermostatic temperature bath was used. They found that at low concentration and low pH the coal water slurry behave pseudo plastic nature and with the increase in ash content and acidic medium viscosity of coal water slurry (CWS) increases.

Lei et al. (2002) examined the sedimentation stability and rheological properties by the use of four types of settling additives namely carboxymethyl cellulose, rhamsan gums, naphthalenesulfonate– formaldehyde condensate (NSF) and xanthan gum. The fly ash released from the Matsuura Power Station on Kyushu Island (Japan) was used as a part of this study. Fly ash was blended with deionized water to make a concentration of 68% by weight. The concentration of added substance naphthalenesulfonate– formaldehyde condensate (NSF) as dispersing agent was set at 0.3% by weight and rhamsan gums (S-194) as a stabilizer at 0.2% by weight. The viscosity of fly ash–water slurries were measured using a rheometer with coaxial rotating cylinder with and without using additives. The temperature of the test sample was kept up at 25°C. The results show that addition of rhamsan gums (S-194) are helpful in increasing stability of the sample. By adding additives, transportation cost increases but system become more stable.

Hiroya et al. (2003) studied the pore defects identified in the slurry and their importance to strengthen the alumina ceramics. They take two slurry samples - First dispersed slurry and second flocculated slurry. They found presence of large pores and dimples in the particles made from the dispersed slurry, while there is no dimple structure was found in the particle made from flocculated slurry. With the help of these pores and dimple found in the slurry, the difference in the slurry strength was explained which shows the alumina ceramics produced from flocculated slurry had a higher average strength than those produce from dispersed slurry.

Dincer et al. (2003) studied rheology of bituminous Turkish coal water slurries by adding naphthalenesulfonate– formaldehyde condensate (NSF) and polyisoprene sulphonic acidic soda, as dispersing agent and sodium salt of carboxymethyl cellulose (CMC-Na) as the stabilizer. The coal sample of Zonguldak area was used for the investigation after mean particle size distribution of 62 μm. The viscosity estimations were done using RVD2-Brookfield pivoting type viscometer. It was found that viscosity by adding dispersing agent at concentration of 0.13% by weight is 1000cp and the stability of the coal water mixture increase by the addition of stabilizing agent at a concentration of 0.01% by weight.

Boylu et al. (2004) studied the effect of volume fraction and particle size distribution on rheology of coal water slurry of different ranks. Two coal sample from Turkey and

one from Serbia was used for the investigation. They used different particle size (d_{50})19, 35 and 50 μm to determine the effect of apparent viscosity. They found viscosity decreased from lower to higher rank coals. For all three samples volume fraction values increases with increase in mean particle size.

Park et al. (2005) investigated the rheological properties of mineral admixtures (MA) (fly ash, blast furnace slag and silica fume) using a rheometer with a cylindrical spindle. The three different systems were made and designated as one, two and three components systems. Mineral admixture is replaced with cement. For the one-component system, rheological properties were improved by adding superplasticizer. Its viscosity and yield stress decreased by replacing cement with fly ash and blast furnace slag while viscosity and yield stress slightly increased by adding silica fumes in the two component system. In the three component system the rheological properties improved both by adding blast furnace slag and fly ash in place of cement.

Ferraris et al. (2005) studied rheological properties of cement paste mixture containing mineral admixtures. Metakaolin (MK), ultrafine fly ash (UFFA), and silica fumes (SF) mineral admixtures added to the cement paste and was concluded that mixtures with ultrafine fly ash (UFFA) gives the best rheological properties and the mixture with silica fumes (SF) gives the worst result. UFFA improved the concrete flow without decreasing the hardness but increasing the cost.

Yuchi et al. (2005) studied the impacts of coal attributes on the properties of coal water slurry. Sixteen different coals of distinctive positions from low carbon contents to high carbon contents were used as a part of the study. Sodium naphthalene sulfonate formaldehyde condensate was chosen as a dispersant. The viscosity was measured by a NXS-11 revolution viscometer . The shear rate was taken between 3.18 to 113.5 s^{-1} at 25°C. They found that the slurryability decreases with increase in solid concentration.

Senapati et al. (2008) examined the rheological behaviour of coal water slurry using natural additives. Two sorts of coal having distinct ash content were acquired from Talcher Coal Field, Orissa, India. The rheological experiment were done using HAAKE RV 30 rotational viscometer. The coal water slurries were arranged with concentration

between 55-63.7 % by weight. The concentrations of additive were taken between 0.4–1.2% by weight. The static stability was measured using rod penetration test. They found that the coal water slurry in the vicinity of naturally added substance showed bingham plastic nature.

Shukla et al. (2008) studied the rheological properties of coal-water-oil mixtures with coal particles of different sizes (108, 75.7 and 62.9 μm). The rheological properties were measured with the help of coaxial cylindrical viscometer at 30° C. The solids concentration and shear rate was varied from 10 -50 % by weight and 100 – 2500 rpm respectively. They found that depending on the concentration of oil and water, the mixtures behaved as pseudo plastic, dilatants and Newtonian fluid. Also a general correlation was developed for the prediction of apparent viscosity of coal-water-oil mixtures.

Mosa et al. (2008) examined the effect of chemical additives or reagents on rheological characteristics of coal water slurry (CWS). Apparent viscosity and flow properties of coal water slurry are sensitive to the use of chemical additives (dispersants and stabilizers). Among studied dispersing agents, sulphonic acid recorded the best performance in modification and reducing CWS viscosity. The best dosage of all tested dispersants was found to be as 0.75 % by wt of solids. With regard to studied stabilizers, Na- CMC recorded better performance than xanthan gum. The best dosage of investigated stabilizers was found to be as 0.1 % by wt. from total solids.

Das et al. (2008) developed a natural additive using saponin from the fruit of the Sapindous laurifolia plant. They examined the rheological qualities of coal water slurry as a component of pH, ash content of coal, coal stacking, measure of saponin and temperature. The coal sample gathered were from Talcher coal fields, Orissa. The rheological experiment were performed using HAAKE (Model RV 30) rotational viscometer. The slurry arranged had weight concentration from 55 to 64% by weight with distilled water. The added substance concentration were varried from 0.4-1.2% by weight. They found that coal-water slurry containing 64 % weight fraction could be achieved in the presence of 0.8 % of saponin.

Zhou et al. **(2010)** studied the rheological characteristics of coal-water slurry. Coal slurry prepared with concentration of 64% by weight and dispersant dosage of 0.7% by weight shows shear-thinning characteristic while with dispersant dosage of 1.5% by weight shows shear-thickening characteristic. The effect of solid content of CWS also studied, result showed that CWS behaves as pseudoplastic characteristic with increase in concentration while behaves as dilatant flow characteristic with increase in dispersant dosage.

Agudo et al. (2010) examined flow behaviour of lime putties acquired after hydration of hard and soft burnt quick limes (CaO) which is examined and compared with the difference found in morphology, molecule size, fractal nature with time and level of accumulation. They found that for the hard burnt lime, lime putty behave as non-Newtonian fluid with thixotropic nature while for soft burnt lime, lime putty behave as non-Newtonian fluid with rheopectic nature. After hydration, best rheological propertieswere achieved for hard burnt lime. This putty become more reactive towards carbonation by smaller particle size and higher surface area. These result were helpful for the prepareness of lime mortars used as a part of the preservation of historical buildings.

Bentz et.al (2012) studied the impact of particle size distribution of fly ash, cement and ratio of fly ash to cement on the viscosity and yield stress of mixed paste. Rheological properties of the arranged cement pastes were analysed using a rotational rheometer. From the experiment, they analysed that rheological properties were influenced by both particle surface area and particle densities decided from measured particle size distribution. Their experiment also revels that yield stress depends on the molecule thickness of the cement components. Cement particle number density decreases by fly ash which acting as a diluent agent. Author likewise inferred that viscosities are affected by both concrete and fly ash particles, with estimated linear relationship between viscosity and surface area or particle density.

Buranasrisak et al. (2012) examined the impacts of particle size distribution and packing qualities on the rheological behaviour of coal-water slurry. A sub-bituminous coal of Indonesian origin was used to set up the experiment. The examples were grouped into six particle size ranges < 38, 38-63, 63-75, 75-90, 90-180 and 180-250

μm. Naphthalene Sulfonate formaldehyde (NSF) and carboxymethyl cellulose (CMC-Na) were used as the dispersive agent and stabilizer respectively. The viscosities of coal water slurries were measured using MV-2000 arrangement II Rotary Viscometer at different solid concentration between 60 to 65 % by weight. The different packing properties of the coal specimens were characterized by making monomodal, bimodal and multimodal appropriations at different course to fine proportions. They observed that most extreme coal stacking was conceivable when coal water slurry was produced using bimodal particle size distribution.

Marcos et al. (2013) studied the effect of rheological behaviour on the ultrafine grinding of an iron ore slurry. They conducted test at different pH (7.3, 8.5 and 10.0) level. Result found that increase in pH increase the slurry dispersion degree but decreases the yield stress and viscosity. So they added sodium hydroxide and lime in the previous processing steps which increases the specific energy consumption, with significant increase in yield stress and viscosity.

Toru et al. (2013) studied the thermal conductivity of high porosity alumina refractory bricks made foaming and slurry gelation method. For application of refractory bricks, its high thermal conductivity must be reduced by increasing the porosity. A GS (gelation of slurry) method is used for this. They prepare the alumina foam and measured porosity, mechanical properties, and thermal conductivity. The results show that this method can successfully produce ceramic foams with porosity from 94 to 98%, and can thus produce high porosity ceramic foams that have low thermal conductivity.

Kirk et al. (2013) studied that impact of binary mixtures of fly ash and limestone and ternary mixtures of fly ash, limestone and metakaolin on the rheological properties of cement pastes. To predict the material behaviour, Bingham model for fluid suspensions was used. They found that plastic viscosity and yield stress were remain unchanged or decreased by replacing ordinary Portland cement (OPC) by coarse limestone powder both for binary and ternary mixtures.

Chen et al. (2014) added limestone fines in place of cement paste to reduce sorptivity and water permeability concrete. The addition of limestone, fills the voids between particles and can reduce the volume of cement paste needed to produce concrete. They

evaluate the effects on the water resistance of concrete, also tested certain properties like workability, strength, water permeability, sorptivity and porosity. It was found that the addition of limestone as cement paste replacement would certainly improve the dimensional stability, strength and substantially improve the water resistance of the concrete produced.

Seddik et al. (2014) studied the concrete formation by the use of binary and composite limestone cement. Objective of study is to design a concrete with low environmental impact using various types and proportions of cementitious materials. Different materials namely, silica fumes, limestone, slag, metakaolin and fly ash were used in various proportions to produce binders. After mixing, a slump test was performed, and concrete was cast into molds (prisms, cylinders and cubes) in three layers and compacted using a plate vibrator and measures certain properties like Mechanical properties, Shrinkage, Carbonation etc.

Singh et al. (2015) studied the rheological behaviour of coal water slurry using Anton Paar Rheolab QC rheometer at 25°C, by varying particle size and concentration. They took particle size <75 μm for the investigation of rheological behaviour of coal slurry and found that concentration have major effect on the rheological behaviour of slurry suspension. As the solid concentration increases, viscosity of coal slurry mixture increases and mixture behave as a non-Newtonian fluid. The rheological behaviour of slurry also analysed by blending mixture of fine particle of 53-75 μm and course particles of 106-150 μm or 150-250 μm with various proportions. It was found that upto a certain extent, viscosity of the slurry decreases with increase in percentage of coarse particle and then increases with increase in fraction of coarse particles.

CHAPTER 3

CHARACTERIZATION OF MINERAL SAMPLE

Four samples of mineral (Iron ore hematite, zinc ore, iron ore magnetite and lime) each varying in their microstructure were obtained from different sources. The different sources of finding of Mineral samples were mines and mineral traders. Throughout this thesis, the four mineral samples are labelled as S-I, S-II, S-III and S-IV for Iron ore hematite, zinc ore, iron ore magnetite, and lime respectively. The various characterization studies that were done on the mineral sample included particle size distribution, pH at different solids concentrations, Scanning Electron Microscopy (SEM) analysis, Energy Dispersive Spectroscopy (EDS) analysis, ternary diagram formation, X-ray diffractogram (XRD) analysis and Fourier transform infrared spectroscopy (FTIR).

3.1 PARTICLE SIZE DISTRIBUTION

The particle size investigation is an endeavor to focus the relative properties of the diverse grain sizes that make up the specimen. It is impractical to focus the individual molecule sizes, however the test can just focus the surmised size range between two sieves. The particle size examination does not give any data on the state of the particles, whether they are rounded or angular.

The particle size distributions of sample S-I, S-II, S-III, S-IV are given in Table 3.1 and shown in Figure 3.1. From Figure, it is observed that the biggest particle size of samples is 500 µm. Result shows that 90.91 % of sample S-I is finer than 250 µm, 72.21% is lies between 106-150 µm and 58.61% sample is finer than 75 µm. while in sample S-II, 61.50% of sample is finer than 250 µm, 42.93% lies between 106-150 µm and 31.68% is finer than 75 µm. In sample S-III, 59.45% of sample is finer than 250 µm, 25.54% lies between 106-150 µm and 9.67% is finer than 75 µm. In sample S-IV, 94.94% of sample is finer than 250 µm, 87.61% lies between 106-150 µm and 57.69% of sample is finer than 75 µm.

3.1.1 Procedure for the particle size analysis

1. Determine the mass of the sample precisely to 100 gm (W).

2. Set up a stack of sieves. A sieve with larger openings is placed above a sieve with smaller openings. A bottom pan should be placed under sieve which has smallest opening

3. Empty the specimen into the stack of sieves from the top.

4. Place the cover on the top of the stack of sieves.

5. Run the stack of sieves through a sieve shaker for around 10 to 15 minutes.

6. Stop the sieve shaker and remove the stack of sieves.

7. Measure the amount of sample held on every sieve and the bottom pan.

3.2 POTENTIAL OF HYDROGEN (pH) OF SLURRY

The pH test method is used to check the aqueous solution of slurry whether the slurry is acidic or basic. The pH in chemistry is the negative log of the hydrogen ions in a solution. Aqueous solutions with a pH value less than 7 are said to be acidic and greater than 7 are alkaline or basics. In pH value 7 is for pure water, called as neutral solution. The pH testing of mineral slurry at different concentration were tested at chemical laboratory at Thapar University, Patiala. The pH was measured by a digital pH meter. The pH meter was first calibrated by dipping the electrode into the buffer solutions and then the electrode was cleaned with distilled water to ensure correct measurements

The pH value of the slurry determined at 20, 30, 40 and 50% concentration by weight shown in the figure 3.2. The pH value of sample S-I, S-II, S-III and S-IV get reduce from 8.83 to 8.09, 6.45 to 5.36, 8.87 to 7.99 and 12.92 to 12.45 respectively with increase in concentration from 20 to 50% by weight.

3.3 SCANNING ELECTRON MICROSCOPE (SEM) / ENERGY DISPERSIVE MICROSCOPE (EDS)

SEM/EDS method is used for the imaging of various types of materials, chemical analysis and surface analysis. SEM equipment is equipped with an EDS. This method provide analytical result of fine or minute particles and also use for the chemical analysis results. By this method we can detect approximate 90 elements with low atomic number. The equipment used was SEM-JSM-6510LV JEOL. In this technique a high energy beam of electrons is made incident on the sample to be analyzed. These energetic electrons then interact with the atoms of the sample and produce different signals that are detected by the sensors.

SEM/EDS is used for analytical result of fine or minute particles and for the imaging of various types of materials, chemical analysis and surface analysis. The scanning electron micrographs (SEM) of the samples at ×1000 magnification are shown in Figure 3.3. Analysis showed that iron ore is of oolitic shaped structure. This oolitic shape consists of oxides and silicates of iron. It is a combination of concentric-botryoidal and radial structure. The dark portion of the sample were mostly Fe_2O_3 and the bright portion were Ti and Si present in magnetite. Chemical composition of ore include Fe_2O_3 (hematite), Fe_3O_3 (magnetite), SiO_2, TiO_2, Al_2O_3. Titanium is present as slag inclusion and this slug inclusion would increase the Titanium contents. EDS results at different point shows that iron minerals in the ore are associated closely with gangue minerals, and elements Fe and O are evenly distributed in the whole surface. Detailed examination of the internal structure of an oolitic unit found that phosphorite grew in successive layers in hematite and thus the phosphorite had a layered or "onion skin" structure in the oolitc unit.

The EDS spectrum analysis gives the composition of the various elements and compounds present in the samples. The detail compositions of the elements and compounds are shown in the table 3.3 and 3.4. EDS shows peaks in spectrum subsequent to the various elements of sample S-I are oxygen (O) 30.45% and iron (Fe) 61.84%. The peaks show these elements are present in immense proportions in sample S-I. Other elements like carbon (C), and titanium (Ti) are present in minor proportion with 3.80 and 3.91% respectively. Presence of carbon (C), iron (Fe), aluminium (Al), Silicon (Si), sulphur(S) and zinc (Zn) are found with proportion 6.11, 6.16, 10.20, 14.32, 4.32 and 5.84% respectively in sample S-II. Spectrum of S-III shows Iron (Fe), oxygen (O), carbon (C), silicon (Si) are found in major proportion with 31.57, 46.47, 9.94 and 7.71% respectively and Sodium (Na), magnesium (Mg), aluminium (Al) are found in minor proportion with 1.51, 1.45, and 1.07% respectively. Spectrum of sample S-IV shows carbon (C), oxygen (O), magnesium (Mg), and calcium (Ca) are present with 21.77, 65.37, 8.62 and 4.23% respectively.

EDS shows peaks in spectrum subsequent to the various compounds of sample S-I are Co_2, TiO_2 and FeO with 13.93, 6.51 and 79.56% respectively. Presence of CO_2, FeO, Al_2O_3, SiO_2, SO_3 and ZnO with proportion 22.40, 7.92, 19.18, 30.63, 10.79 and 7.27% respectively are found in sample S-II. Spectrum of sample S-III shows CO_2, FeO

and SiO_2 with proportion 36.42, 40.62 and 16.49% respectively whereas spectrum of sample S-IV shows CO_2, MgO and CaO with proportion 79.78, 14.30 and 5.92% respectively.

The observations from the SEM analysis conducted on the mineral samples showed that the mineral particles were mainly irregular in shape and there was a considerable difference in the distribution of particles of the four mineral samples. Lime and Iron ore (Hematite) sample contained more fine particles than Zinc ore and Iron ore (Magnetite) sample.

3.3.1 Ternary Diagram

Ternary plot is triangular plot or representation of three variables as shown in figure 3.5. It represent the position of compounds in the equilateral triangle. It is used in the mineralogical characterisation to show the composition of material in three compounds system. The advantage is that it is two-dimensional representation of three variable system. Ternary diagram is a representation of three dimensional or more commonly as a two dimensional projection of liquid surface onto the base of triangle created when the three binary diagrams are joined together. The irregular triangle is often transformed into an equilateral triangle to facilitate presentation and interpretation

3.4 X-RAY DIFFRACTION ANALYSIS (XRD)

The mineralogical structure of tests has been assessed by X-ray diffraction (XRD) method. The diffract grams determines the different stages and minerals display in the specimens. The X-ray diffraction pattern of the mineral specimens are gathered by a Philips X'Pert diffractometer (Model: PW 1710), worked at 40 kV and 30 mA using Cu Kα radiation (λ=1.542 Å). The sample is scanned over a scattering angle 2θ from 0±80°. The JCPDS (Joint Committee on Powder Diffraction Standards) data files have been used for identification of the minerals present in the sample.

The XRD results of the sample S-I, S-II, S-III and S-IV are shown in Figure 3.6. From the XRD pattern, it can be seen that iron ore consists of mainly hematite, magnetite, quartz and calcite. The pattern demonstrates that hematite reduces to magnetite which made specimen to be isolated by low power magnetic separation. The peak of calcite getting lower which shows the decomposition of $CaCO_3$ and kaolinite was disappeared. In the iron mineral (magnetite) sample magnetite is the primary

component yet quartz additionally existed which demonstrates that iron and quartz were fine-scattered together and is difficult to isolated. XRD pattern peaks can be promptly distinguished as face-center cubic phase, pattern did not affirms the high purity of product. Diffraction pattern shows the strong and sharp reflection peaks of iron ore (magnetite) which shows its crystalline nature. The most strong peak of hematite (Fe_2O_3) is in close proximity to 2θ=33.1618° with d-spacing 2.69931 Å and the quartz (SiO_2) is in close proximity to 2θ= 26.8036° with d-spacing 3.32343 Å is found in sample S-I, and in sample S-II, Zinc Sulfide (ZnS) is in close proximity to 2θ= 28.5208° with d-spacing 3.12711 Å and the quartz (SiO_2) is in close proximity to 2θ=26.6344 Å with d-spacing 3.34415 Å is found. Whereas most string peak of Magnetite (Fe_3O_4) is in close proximity to 2θ= 57.0453° with d-spacing 1.61317 Å and the quartz (SiO_2) is in close proximity to 2θ= 53.4908° with d-spacing 1.71167 Å is found in sample S-III. In sample S-IV, magnesium calcium bis(carbonate) [MgCa(CO3)2] is in close proximity to 2θ= 30.9482° with d-spacing 2.88715 Å.

3.5 FOURIER TRANSFORM INFRARED SPECTROSCOPY (FTIR)

Fourier transform infrared spectroscopy is a technique to obtain infrared spectrum of absorption emission of solid, liquid or gas. The overall internal energy of a molecule in a first approximation can be determined by the sum of rotational, vibrational and electronic energy levels. Infrared spectroscopy is the investigation of communications between matter and electromagnetic field in the Infraredregion. In this spectral region, the electromagnetic waves primarily couple with the sub-atomic vibrations. In other words, a molecule can be excited to a higher vibrational state by absorbing IR radiation. . The chances of a specific IR frequency being absorbed relies on the interaction between this frequency and the particle. In general, a frequency will be clearly consumed if its photon energy matches with the vibrational energy levels of the atom. IR spectroscopy is subsequently a capable method which gives unique data on the chemical arrangement of the specimen. In spectroscopy, it is required to know which frequencies are consumed and which are not. This obliges that the radiation source covers a wide spectral range and the individual frequencies of the radiation are analysed.

FTIR spectrometer operates on the principle of Fourier transform and reverse Fourier transform

Expression of Fourier transform:

$$F(\omega) = \int_{-\infty}^{+\infty} f(x) e^{i\omega x} dx$$

(3.1)

Expression of reverse Fourier transform:

$$f(x) = \frac{1}{2\pi} \int_{-\infty}^{+\infty} f(\omega) e^{-i\omega x} d\omega \quad (3.2)$$

Figure 3.7 represents the FTIR spectrum of sample S-I, S-II, S-III and S-IV. Figure shows the spectrum of sample S-I which shows the stretching vibration of aromatic (C-C) at 1491.4 cm^{-1} and the presence of alkyl halides at 551.3 cm^{-1} can be seen. Figure 3.7 represent the spectrum of sample S-II which shows stretching vibration of alcohol (O-H) free hydroxyl at 3620.4 cm^{-1}, (O-H) H-bonded at 3432.5 cm^{-1} and bending primary amines (N-H) at 1623.6 cm^{-1}. Some other stretching vibrations can be seen at 1080.0 cm^{-1} shows the presence of aliphatic amine group (C-N). Presence of alkynes (C(triple bond)C–H) also seen at 699.9 cm^{-1}. Figure shows the spectrum of sample S-III shows the presence of a stretching vibration of alcohol (O-H) at 3749.12 and 3445.11 cm^{-1} also bending primary amines (N-H) at 1626.11 cm^{-1}. Presence of rocky alkanes (C-H) at 1384.11 cm^{-1}. Some other stretching vibrations can be seen at 1075.10 cm^{-1} shows the presence of aliphatic amine group (C-N). Intense peaks at 564 and 468 cm^{-1} can be attributed to the stretching vibration of the Si-O groups and C=O bonds in carboxylic acid respectively. Figure represent the FTIR spectrum of sample S-IV which shows the stretching vibration of alcohol (O-H) at 3643.7 and 3446.28 cm^{-1}, presence of aromatic stretching (C-H) at 2897.31 cm^{-1}, aldehydes (H–C=O) at 2526.29 cm^{-1} and bending primary alkanes (C-H) found at 1441.4 cm^{-1}. Presence of alkyl halides (C–Cl) also found at 727.21 cm^{-1}.

Table 3.1: Particle size distribution

Particle size, (μm)		710	500	355	250	150	106	75	53
% finer	S-I	100	97.8	94.71	90.91	80.01	72.21	58.61	0
	S-II	100	95.15	73.99	61.50	52.08	42.93	31.68	0
	S-III	100	99.03	86.34	59.45	35.74	25.54	9.67	0
	S-IV	100	99.21	98.68	94.94	91.66	87.61	57.69	0

Table 3.2: pH values of mineral samples

Concentration (% by weight)		20%	30%	40%	50%
Sample	S-I	8.83	8.59	8.36	8.09
	S-II	6.45	6.04	5.77	5.36
	S-III	8.87	8.63	8.39	7.99
	S-IV	12.92	12.78	12.63	12.45

Table 3.3: Elements present in samples

Elements		C	O	Ti	Fe	Mg	Ca	Al	Si	S	K	Zn	Na
Sample	S-I	3.80	30.45	3.91	61.84	-	-	-	-	-	-	-	-
	S-II	6.11	51.63	-	6.16	-	-	10.20	14.32	4.32	1.41	5.84	-
	S-III	9.94	46.74	-	31.57	1.45	-	1.07	7.71	-	-	-	1.51
	S-IV	21.77	65.37	-	-	8.62	4.23	-	-	-	-	-	-

Table 3.4: Compounds present in samples

Compounds		Co_2	TiO_2	FeO	MgO	CaO	Al_2O_3	SiO_2	SO_3	K_2O	ZnO	Na_2O
Sample	S-I	13.93	6.51	79.56	-	-	-	-	-	-	-	-
	S-II	22.40	-	7.92	-	-	19.28	30.63	10.79	1.70	7.27	-
	S-III	36.42	-	40.62	2.41	-	2.03	16.49	-	-	-	2.03
	S-IV	79.78	-	-	14.30	5.92	-	-	-	-	-	-

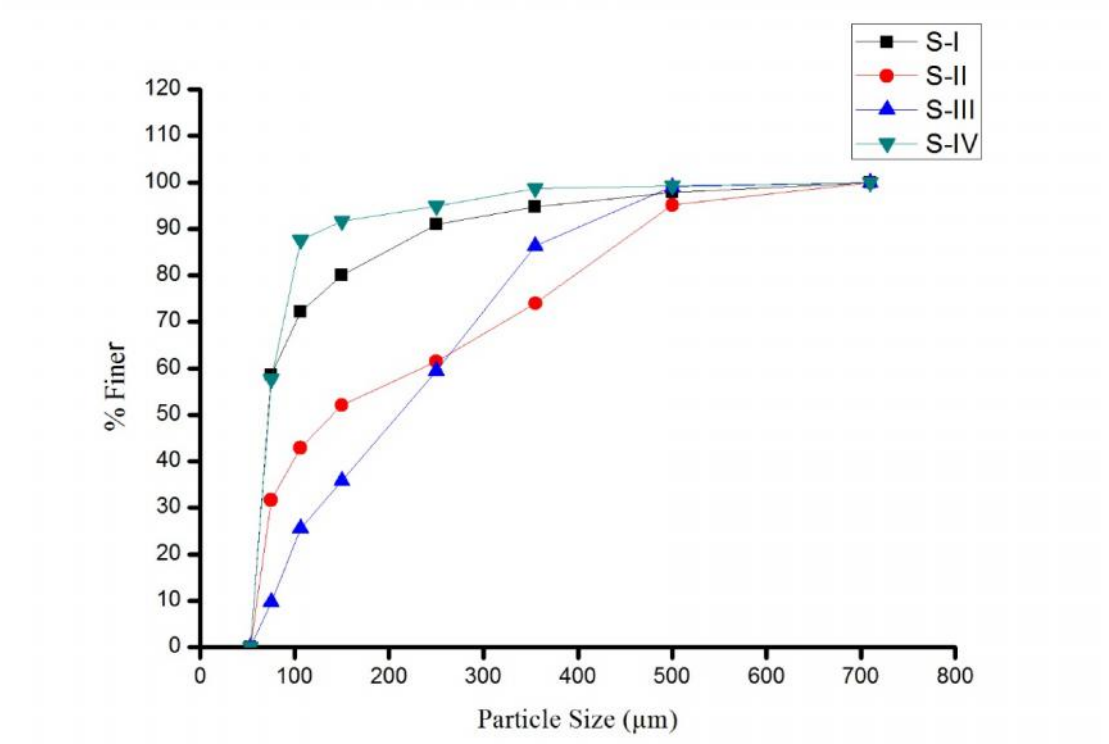

Figure 3.1: Particle size distribution

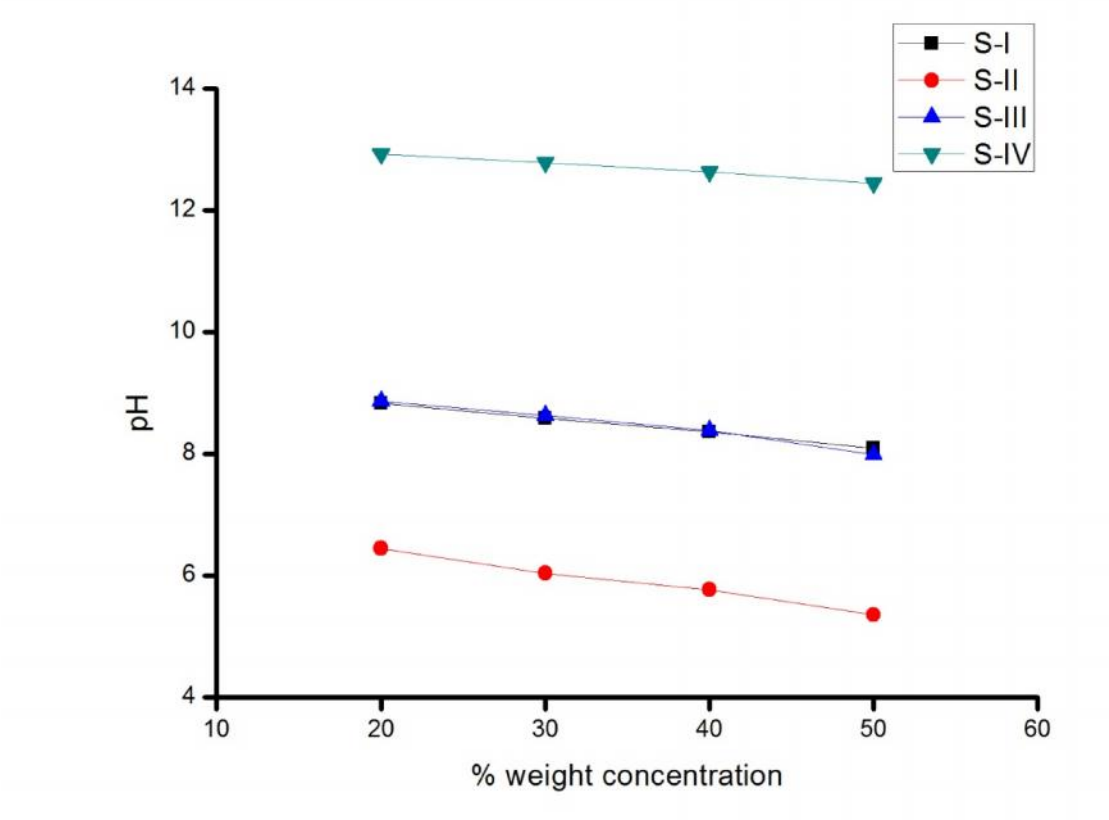

Figure 3.2: pH at different solids concentration (% by weight)

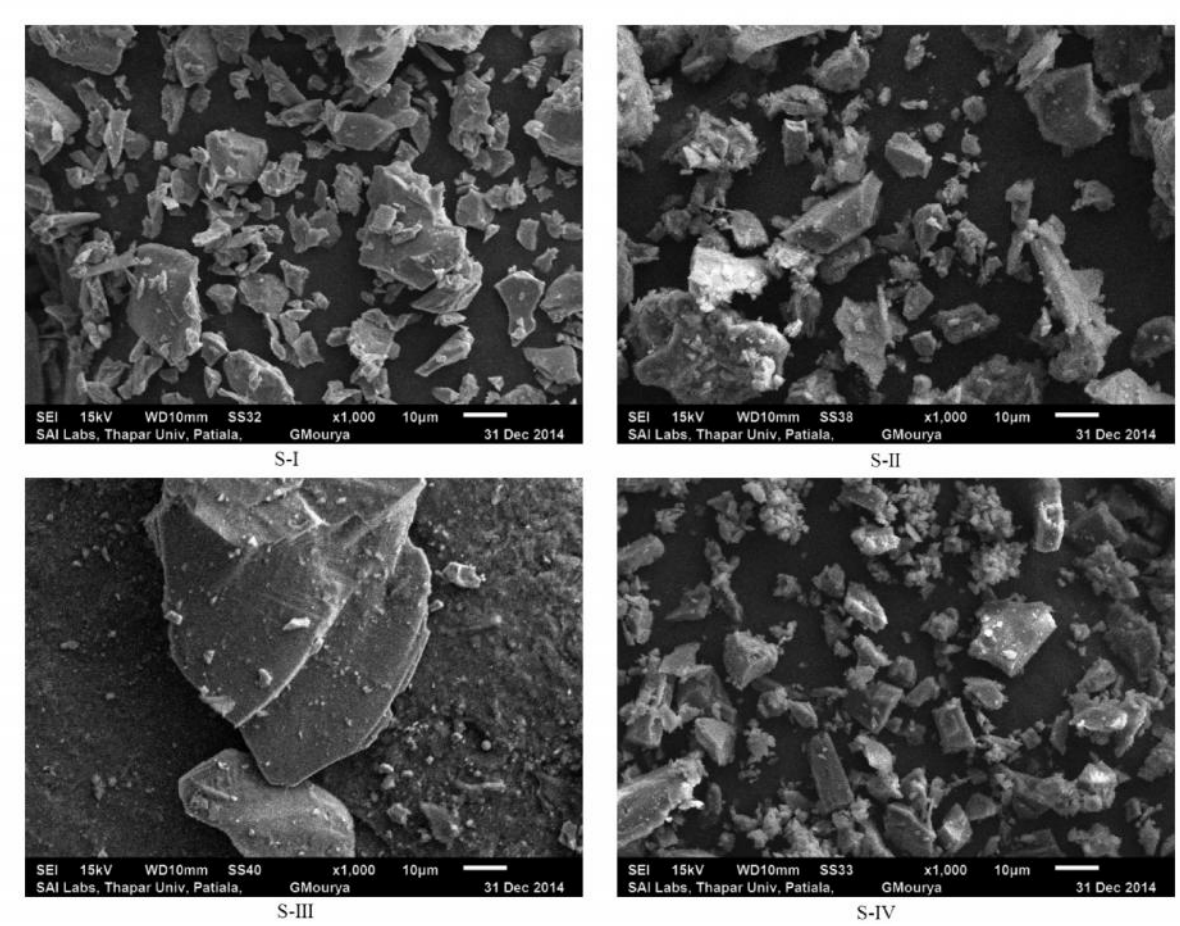

Figure 3.3: Scanning Electron Micrograph of samples

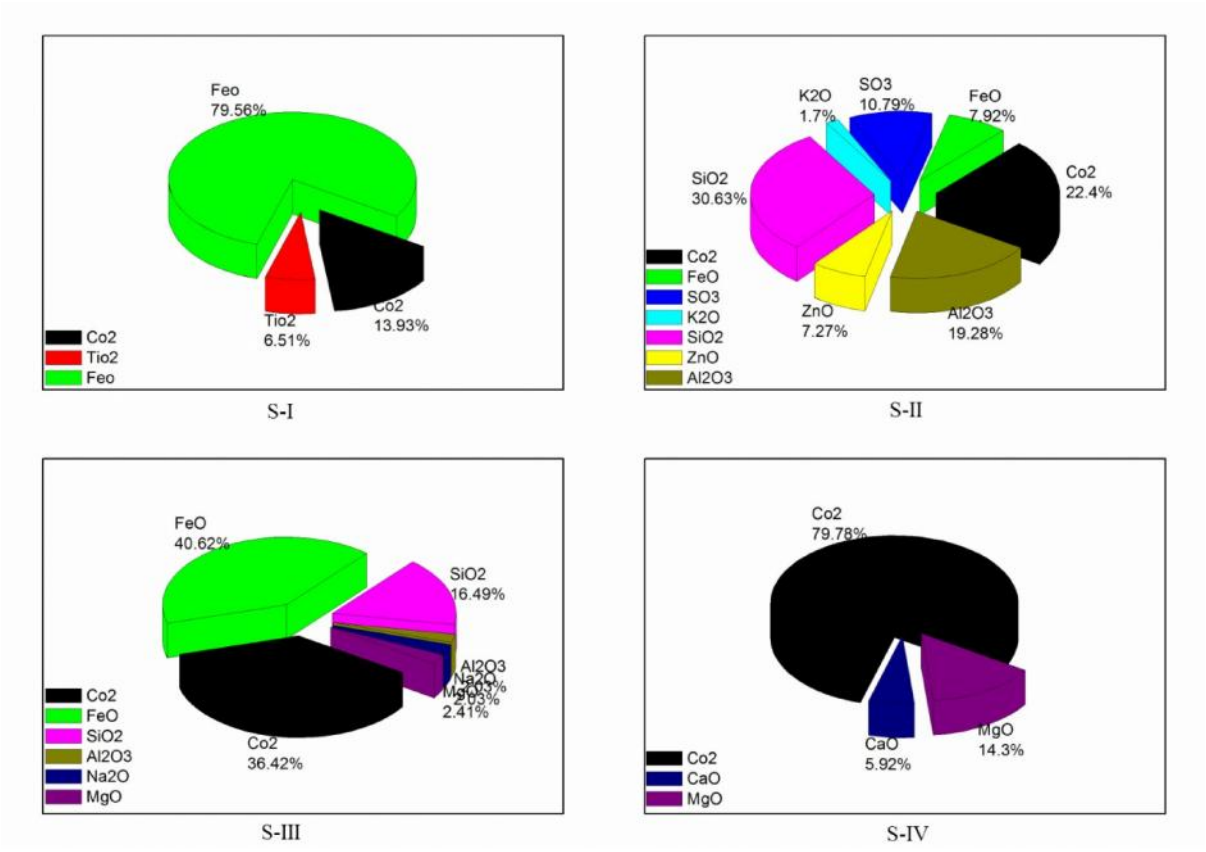

Figure 3.4: Compound (%) of samples

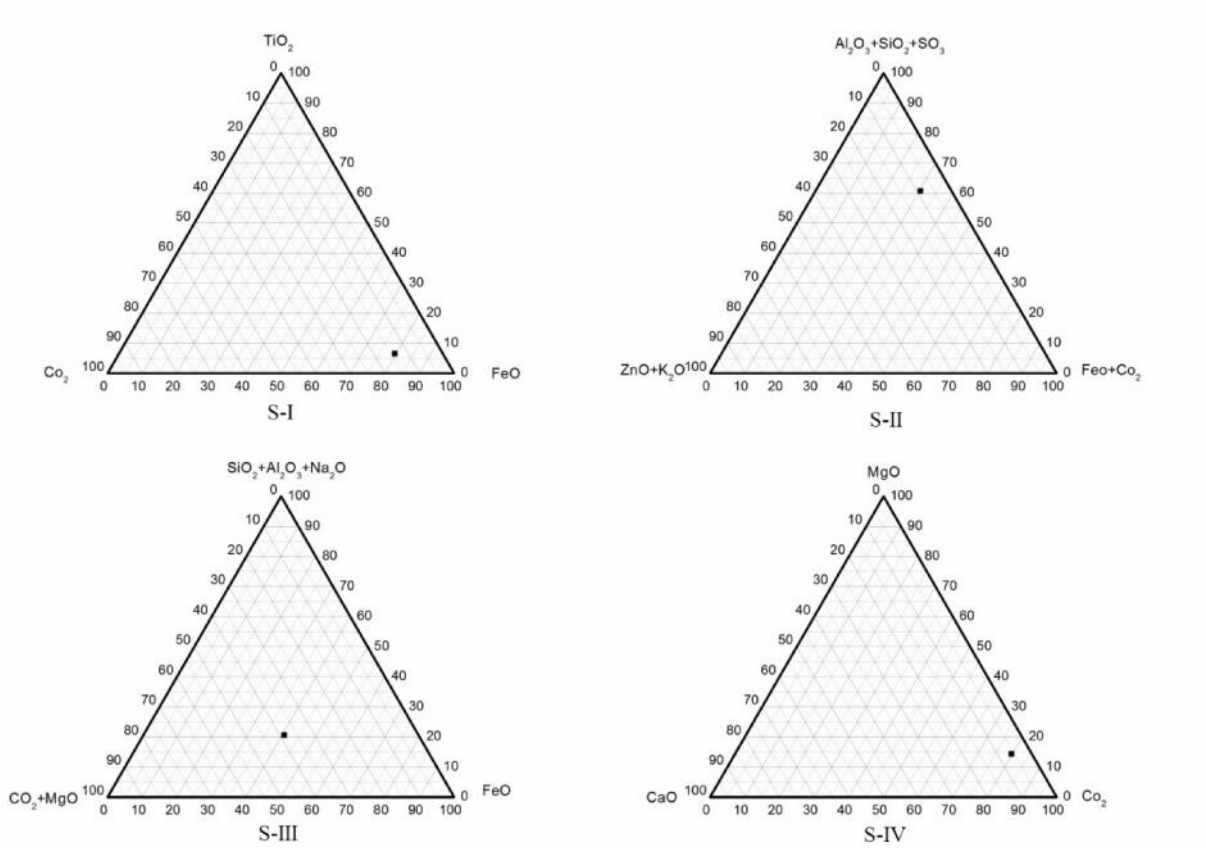

Figure 3.5: Ternary oxide diagram of samples

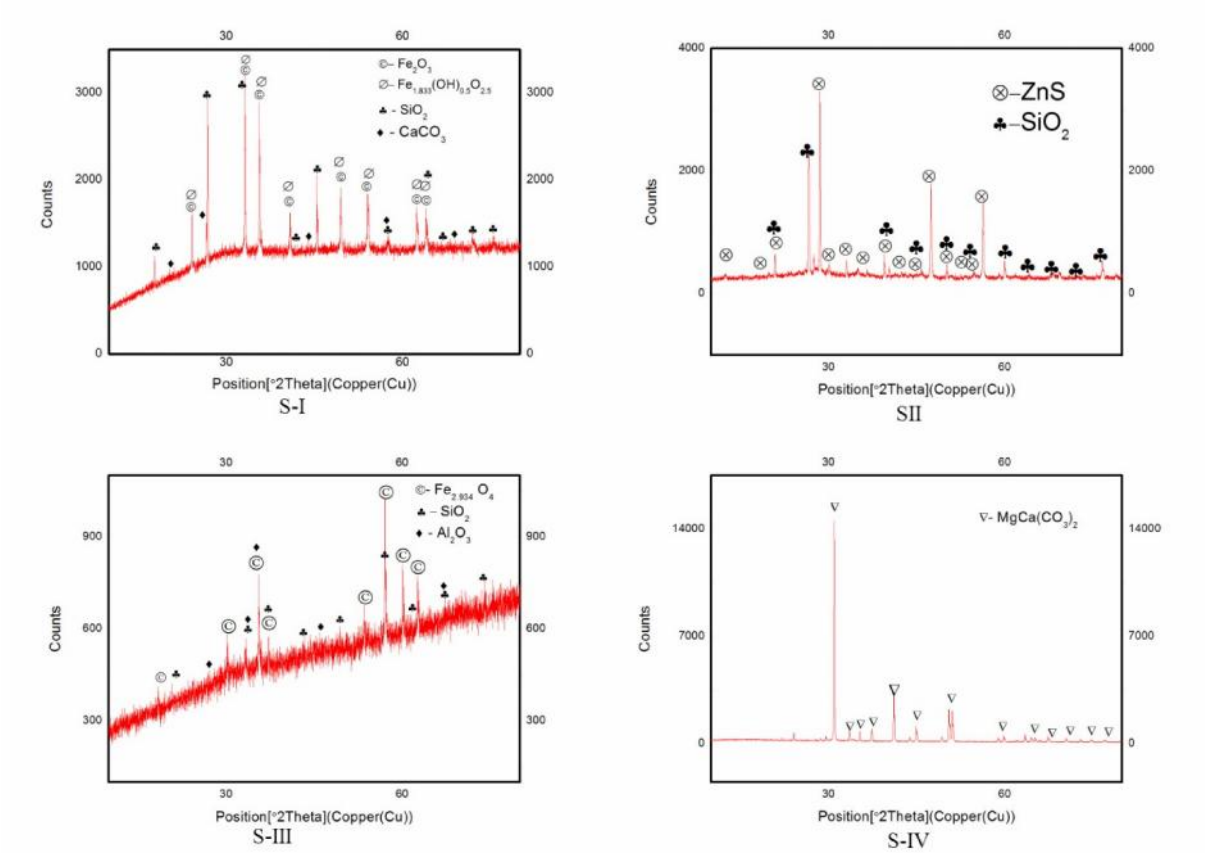

Figure 3.6: X-ray diffractogram of samples

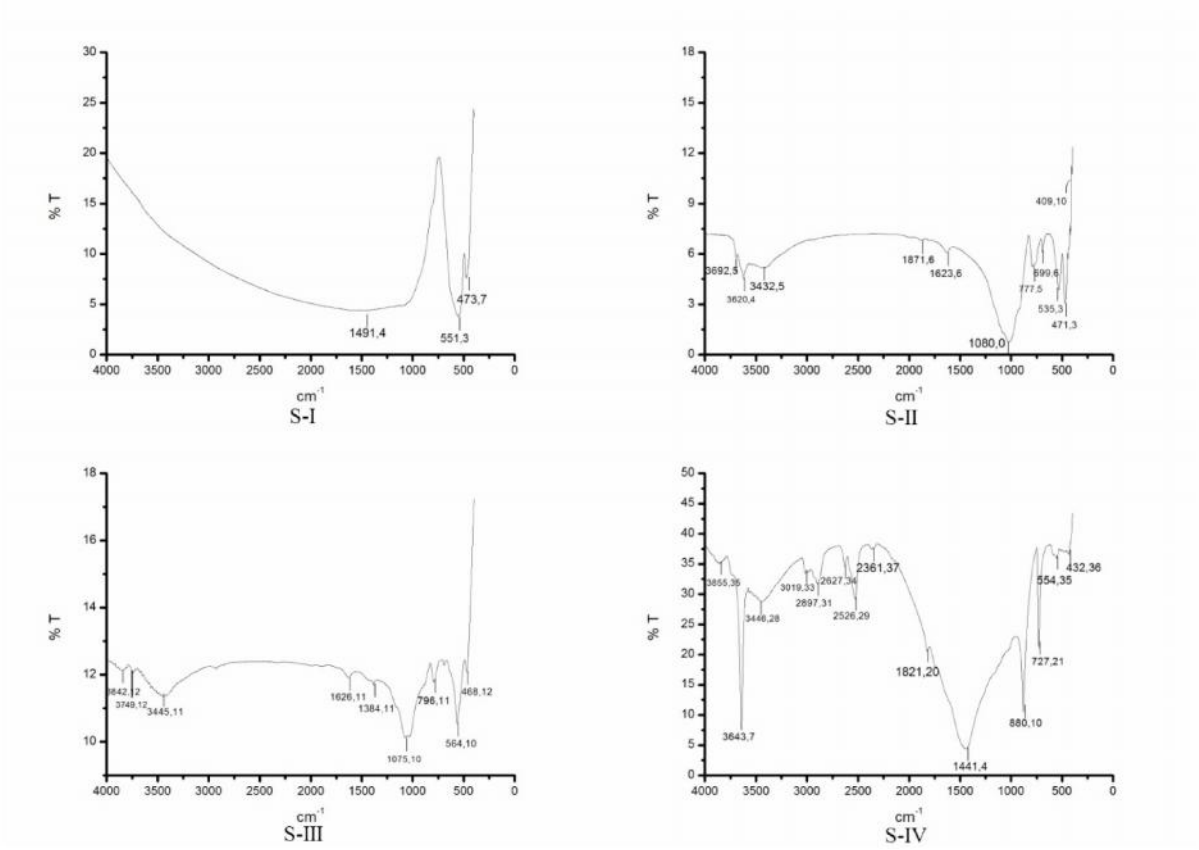

Figure 3.7: Fourier Transform Infrared Spectroscopy Spectrum of samples

CHAPTER 4

RHEOLOGICAL STUDIES ON MINERAL SLURRY

During pipeline transportation of solid particles, the estimation of energy needed for pumping relies on the slurry viscosity. The viscosity of carrier fluid alters by the presence of solid particulates in the carrier fluid depends upon the particle size distribution, pH, specific gravity, settling and concentration of solids present. The rheological studies are extremely valuable for deciding the viscous characteristics of slurry w.r.t. slurry concentration and material properties. In the present study, the rheological experimentation was done on sample S-I and sample S-II. The rheological data was produced by an Anton Paar RheolabQC rheometer.

4.1 DESCRIPTION OF EQUIPMENT

Rheological characteristics of mineral slurry suspension sample S-I and S-II were studied using the Anton Paar Rheolab QC rheometer (Germany) which is available in mechanical engineering department of Thapar University, Patiala. The measurements are obtained by selecting controlled shear rate test settings. It has wide speed and torque ranges and very short motor response time. The measuring systems can be detected automatically by the inbuilt tool master system that ensures the exact measuring data to be used with more precision. The measuring system consists of a spindle having bob and a cup with a small annular gap in between them. The mixture is prepared for each measurement and is filled up to the mark in the measuring cup. The measuring cup is then inserted into the measuring cylinder and the system is coupled to the rotating spindle by pushing down the flanged coupling.

The slurry is subjected to shearing action in between the annular gap between the measuring cup and bob, and hence shear stress is measured as a function of shear rate. The output results are obtained on the Rheoplus software installed on a computer which is connected to the rheometer by LAN connection.

4.2 EXPERIMENTAL PROCEDURE

Measuring system DG42-SN22909/QC-LTD was chosen for the rheological measurements. It was thoroughly cleaned and dried before being used. For the preparation of mixture samples, a known amount of sample was added to a known amount of water, depending on the solid concentration required by weight. Mixture samples were prepared, the mixture was continuously stirred by a glass rod and the time of stirring varied between 5 and 10 minutes. Also appropriate consideration was taken to prevent spillage of mineral slurry mixture.

The amount of sample required for mixture, was weighed in a single pan electronic balance (least count ±0.1mg) for each of the samples. The rheological measurements were made at solids weight concentration of 30, 40 and 50% by weight and at temperature of 25, 35 and 45° C. The shear rate was applied from 0 to 600 s^{-1} for a time of 2 minutes to quantify the relating shear stress under controlled shear rate. The temperature was within the limit of ± 0.5° C and was controlled by using a water bath system. The rheological results were obtained on a computer screen.

4.3 RHEOLOGICAL BEHAVIOUR OF IRON ORE SLURRY

Various characterization methods such as particle size distribution, pH, Scanning Electron Microscopy (SEM) analysis, Energy Dispersive Spectroscopy (EDS) analysis and X-ray diffractogram (XRD) analysis are already discussed in chapter 3. The rheological properties of sample S-I (Iron ore hematite) were determined at different concentrations of 30-50% by weight. The flow characteristics of mineral sample having fine particle size and different particle size distributions were determined by the rheological study. The flow behaviour obtained for fine particle size at different mineral concentration (by weight) is presented in the rheograms 4.1.

4.3.1 Effect of solid concentration and temperature on rheology of Iron ore slurry

From figure 4.1, it is observed that concentration have dominating effect on the rheological behaviour of slurry suspension. Rheogram of sample S-I, shows a linear relation between shear stress and shear rate upto 30% concentration which shows that mixture is of Newtonian nature while above 30% concentration shear thinning starts which shows Pseudoplastic nature. The pseudoplastic nature is explain in equation 4.1.

For equation to be satisfied pseudoplastic nature, yield shear stress should be non-zero ($\tau_y > 0$) and for the Newtonian nature yield shear stress should be zero ($\tau_y = 0$). This is due to the complex structure and deformation effects exhibited by the materials involved in the fluids.

$$\tau = \tau_y + \dot{K}\gamma^{\dot{n}} \tag{4.1}$$

Rheogram of sample S-I at 25°C shown in figure 4.1 shows that up to the shear rate of 150 s^{-1}, rheogram shows linear relation. As the shear rate increases gap between curves increases rapidly. The shear stress value of the sample slurry increases from 7.7 Pa, 15.15 Pa, 22.9 Pa and 34.35 with the concentration of 30, 40, 50 and 60% by weight respectively at the temperature of 25°C. The decrease in the shear stress can be attributed to the increase in the consistency of the slurry suspension, reduced the resistance of shear. When in the suspension larger numbers of solid particles are present, high value of initial shear stress is required to start the shearing process. With increases the temperature, decrease the number of solid particles and surface area per unit volume of the slurry suspension and hence shear stress get reduced.

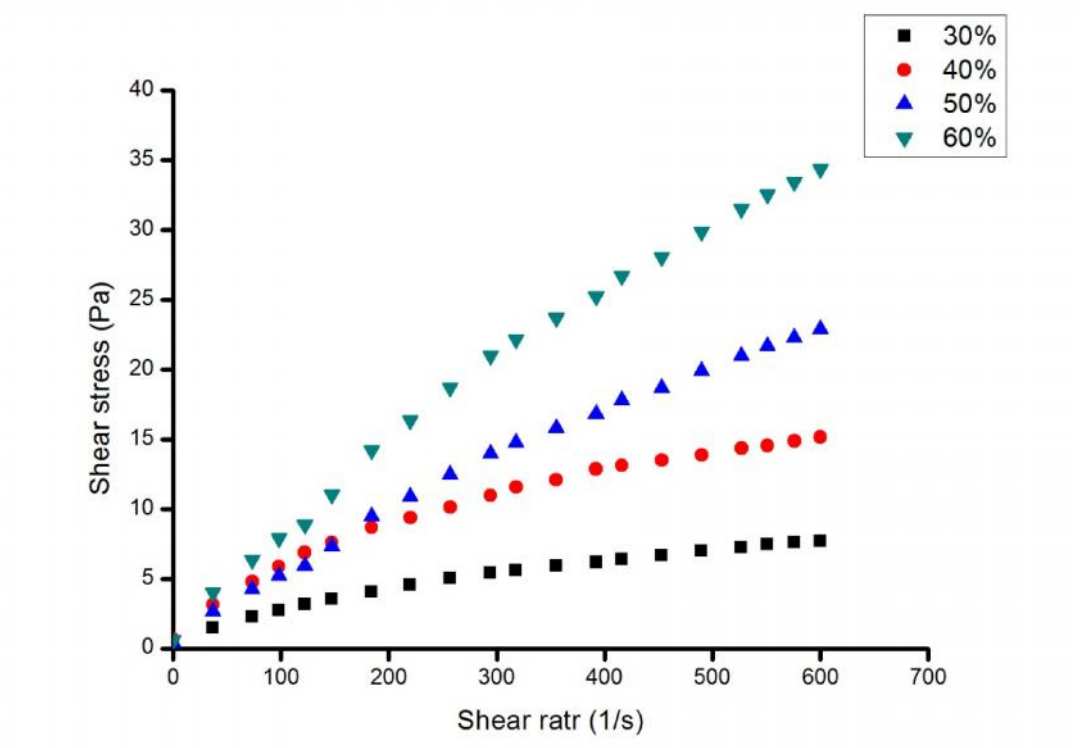

Figure 4.1: Rheogram of sample S-I at different concentrations (% by weight) (25°C)

Rheogram figure 4.2 shows, as temperature increases, slope of the curve decreased. The decrease in slope with increase in temperature can be attributed to the fact that with increase in temperature, the kinetic energy of molecules increases. With increase in kinetic energy, the magnitude of attractive forces between molecules decreases and molecules can now move more freely with respect to one another, which results in lesser viscosity. Rheogram figure 4.2 shows that the shear stress value of the sample slurry decrease from 7.7 Pascal (Pa) to 6.83 Pa , 5.31 Pa and 3.98 Pa with the temperature of 35, 45 and 55°C at the concentration of 30% by weight.

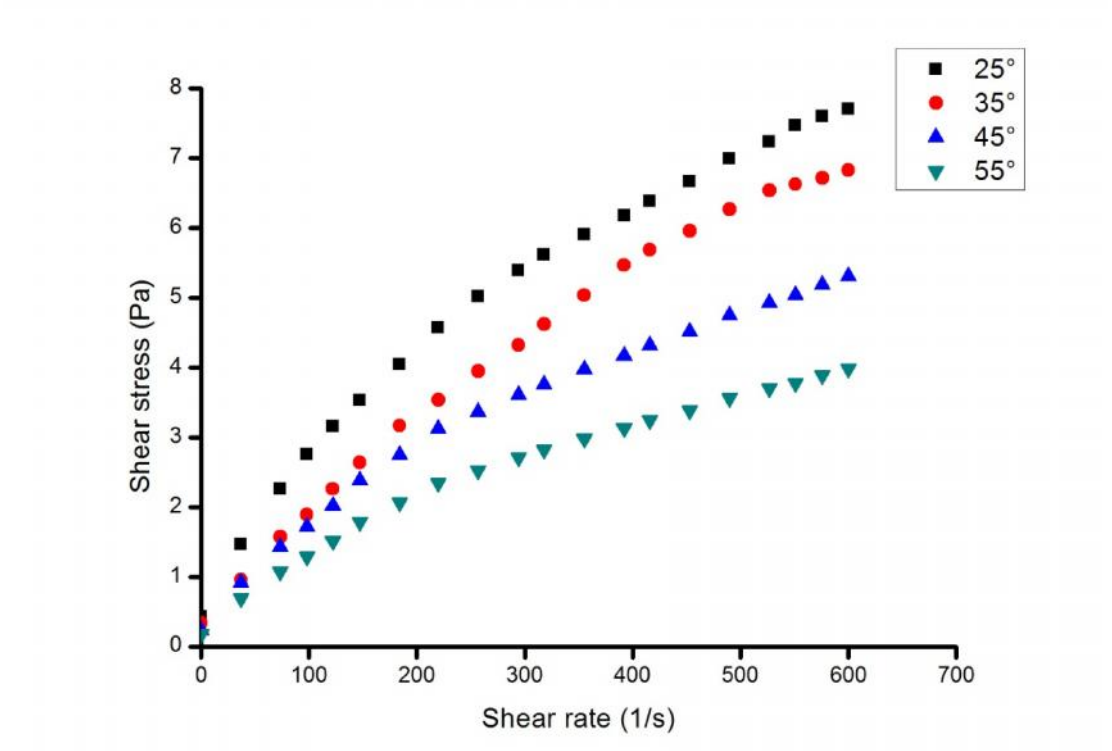

Figure 4.2: Variation of shear stress of sample S-I with temperature for Cw=30%

4.3.2 Variation of apparent viscosity with shear rate and temperature

As the solid concentration increases, viscosity of mineral mixture increases. This can be attributed to the fact that when concentration increases, the density of mineral particles in the mineral mixture also increases, which result in the increase in the

viscosity as particle to particle shear interactions increases. From the figures, it is observed that the viscosity value decreased with increases the temperature of slurry suspension at fixed shear rate. With the increases of slurry concentration from 30 to 60% by weight, the value of viscosity increases.

The dependence of viscosity on solid concentration against shear rate for sample S-1 is shown in Figure 4.3. The shear thinning behaviour or "pseudoplastic" behaviour of the slurry was observed and that the flow pattern of slurry is almost perfectly Newtonian with only a slight degree of shear thinning when the solid concentration of the slurry was less than 40% and that the shear thinning trend of the slurry become more predominant at higher solid concentration. This can be attributed to the viscous forces which dominate at higher shear rates and causes a breakdown of the slurry structure which causes a decrease in the slurry viscosity with an increasing shear rate. At higher shear rates, the viscous forces affect the slurry structure more, causing the slurry structure to become distorted, hence leading to appear shear thinning. Also, the increase in solid loading causes an increase in the viscosity and shear stress of mineral slurry as the inter particle interaction among the minerals particulates highly increases and the effective area under shear also increases.

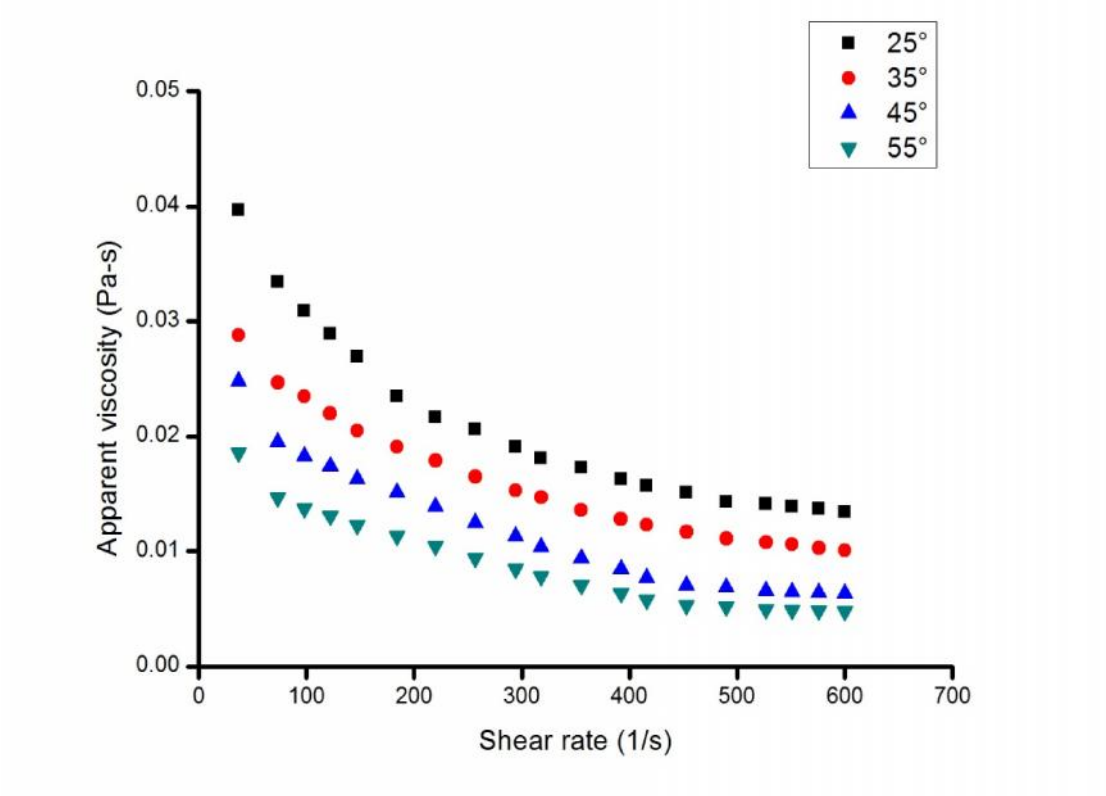

Figure 4.3(a): Variation of apparent viscosity with shear rate of sample S-I at C_w = 30 %

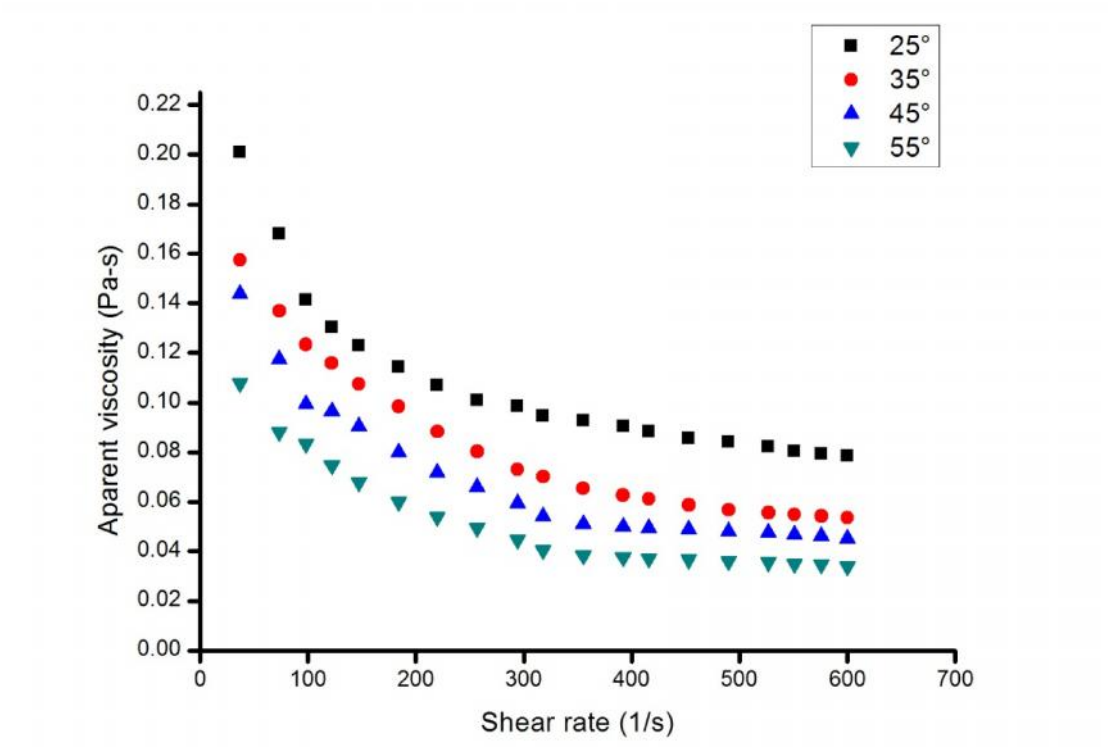

Figure 4.3(b): Variation of apparent viscosity with shear rate of sample S-I at C_w = 60 %

The relative viscosity of slurry suspension with the variation of the temperature is shown in Figure 4.4(a) at 98 s^{-1}. The relative viscosity of the all the slurry suspension decreases with increases the temperature which shows the fundamental properties the any viscous material. With increases the slurry temperature, increased the kinetic energy of the slurry particles promote to reduce the intermolecular forces between adjacent layers which results in decrease in relative viscosity of the slurry suspension. When slurry suspension temperature increases from 25ºC to 35ºC, relative viscosity get reduced 12.66% with 60% concentration, 12.63% with 50% concentration, 13.96% with 40% concentration and 23.94% with 30% concentration respectively. With the increase of slurry temperature from 35ºC to 45ºC, the relative viscosity decrease 19.52%, 11.42%, 14.56% and 22.12% with the 60, 50, 40 and 30% concentration by weight respectively. With the increase of slurry temperature from 45ºC to 55ºC, the relative viscosity decrease 6.14%, 7.81%, 11.43% and 10.67% with the 60, 50, 40 and 30% concentration by weight respectively.

The relative viscosity of slurry suspension with the variation of the temperature is shown in Figure 4.4(b) at 527 s^{-1}. When slurry suspension temperature increases from 25ºC to 35ºC, relative viscosity get reduced 32.56% with 60% concentration, 32.60% with 50% concentration, 28.57% with 40% concentration and 23.40% with 30% concentration respectively. With the increase of slurry temperature from 35ºC to 45ºC, the relative viscosity decrease 14.59%, 16.27%, 36.86% and 39.16% with the 60, 50, 40 and 30% concentration by weight respectively. With the increase of slurry temperature from 45ºC to 55ºC, the relative viscosity decrease 6.11%, 12.34%, 15.43% and 18.37% with the 60, 50, 40 and 30% concentration by weight respectively. Based on the relative viscosity data results in Figure 4.4(a) and 4.4(b), the optimum modification temperature found as 45ºC. The relative viscosity reduction was marginal with increasing the temperature from 45ºC to 55°C for all the test shear rate condition.

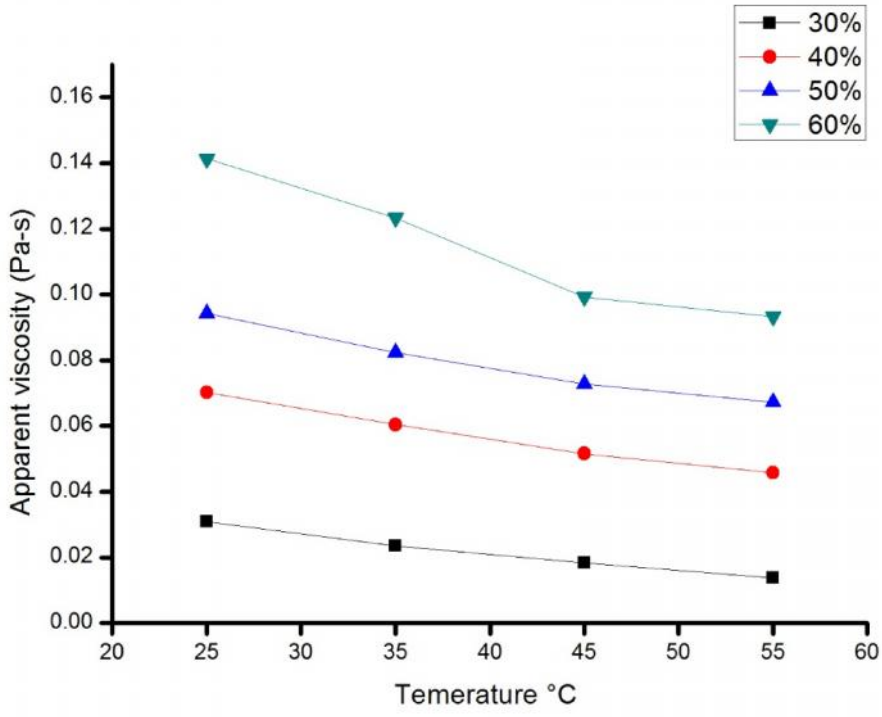

Figure 4.4(a): Variation of apparent viscosity with temperature of sample S-I (98 s^{-1})

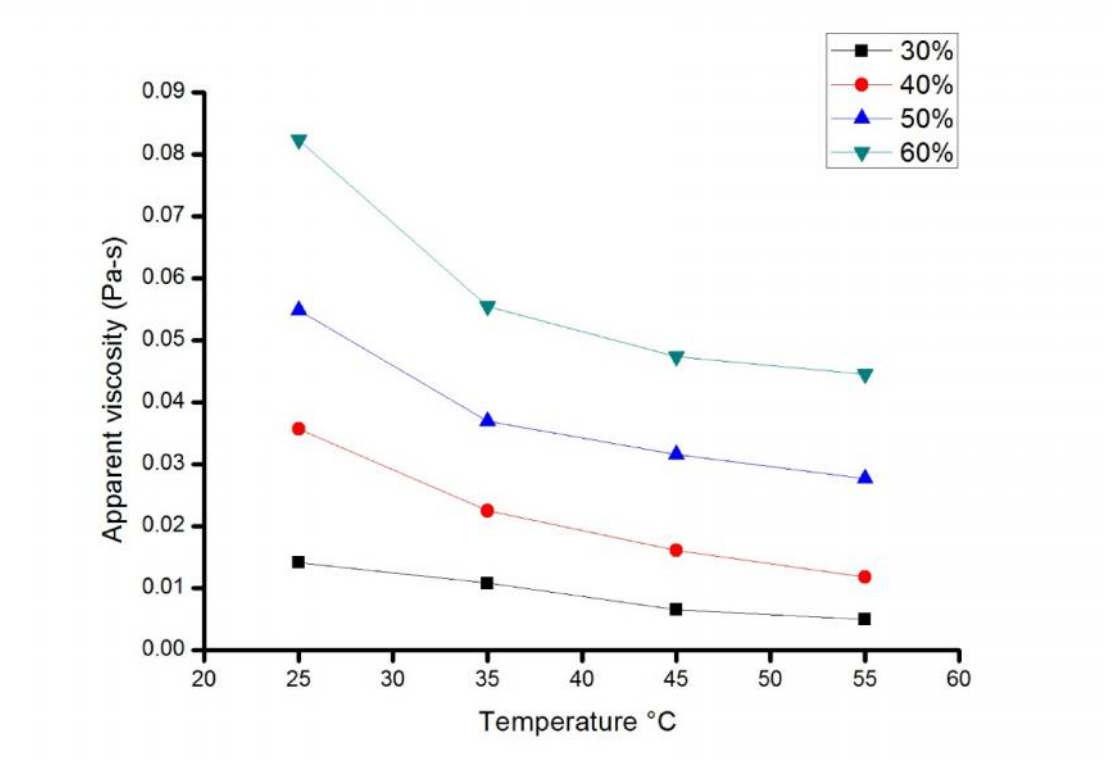

Figure 4.4(b): Variation of apparent viscosity with temperature of sample S-I (527 s^{-1})

4.4 RHEOLOGICAL BEHAVIOUR OF ZINC ORE SLURRY

4.4.1 Effect of solid concentration and temperature on rheology of zinc ore slurry

Figure 4.5 shows the shear stress value of the sample slurry decrease from 3.405 Pascal (Pa) to 2.27 Pa, 1.85 Pa and 0.753 Pa, with the concentration of 60, 50, 40 and 30% by weight respectively at the temperature of 25°C. Rheogram figure 4.6 shows that the shear stress value of the sample slurry decrease from 0.753 Pascal (Pa) to 0.634 Pa, 0,56 Pa and 0.42, with the temperature of 35 ,45 and 55°C at the concentration of 30% by weight.

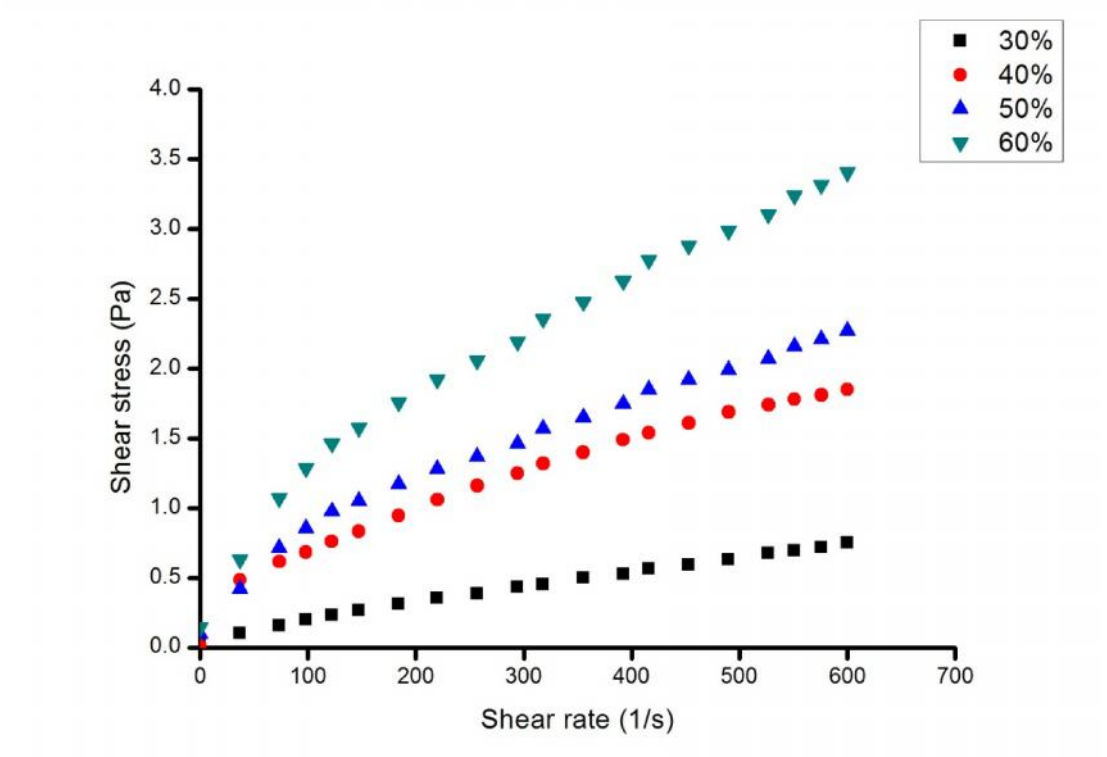

Figure 4.5: Rheogram of sample S-II at different concentrations (% by weight) (25°C)

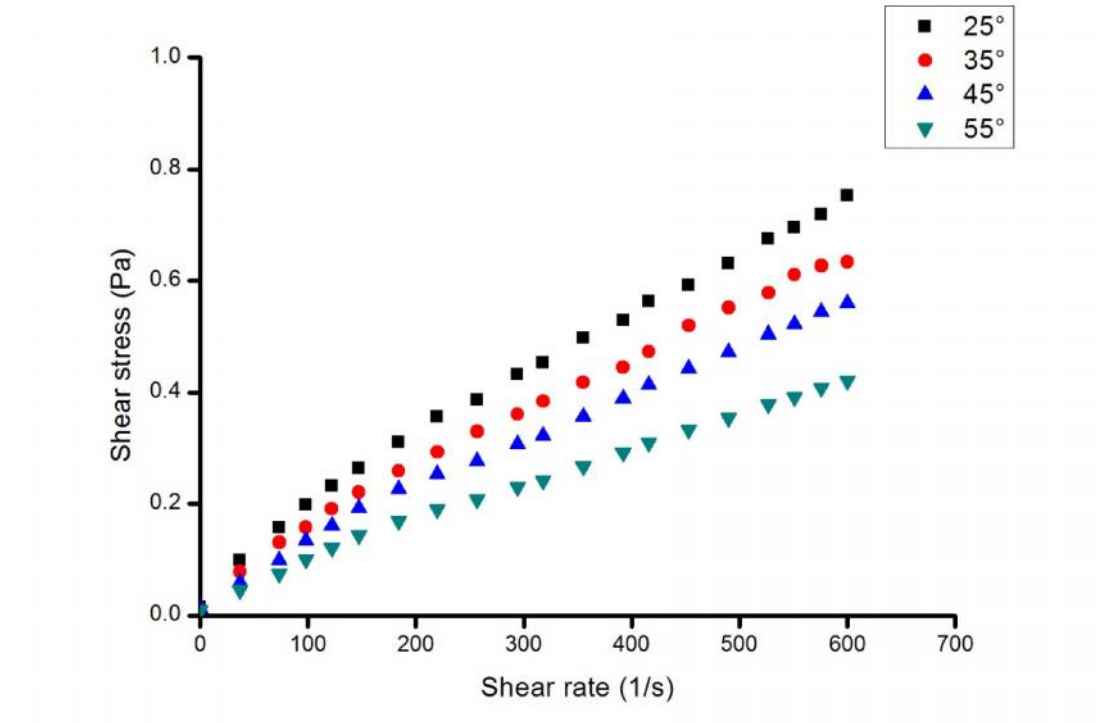

Figure 4.6: Variation of shear stress of sample S-II with temperature for Cw=30%

4.4.2 Variation of apparent viscosity with shear rate and temperature

From the figures, it is observed that the viscosity value decreased with increases the temperature of slurry suspension at fixed shear rate. With the increases of slurry concentration from 30 to 60% by weight, the value of viscosity increases.

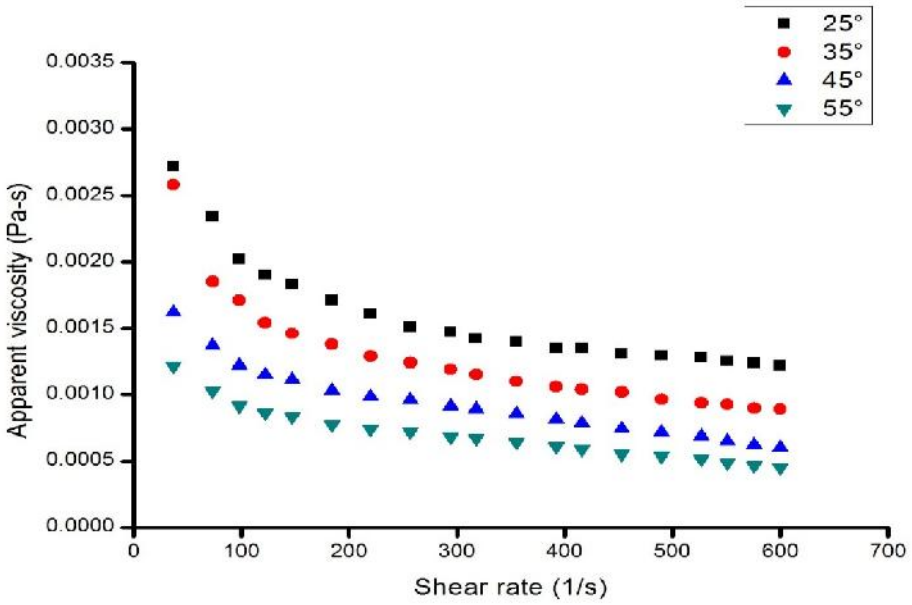

Figure 4.7(a): Variation of apparent viscosity with shear rate of sample S-II at C_w = 30 %

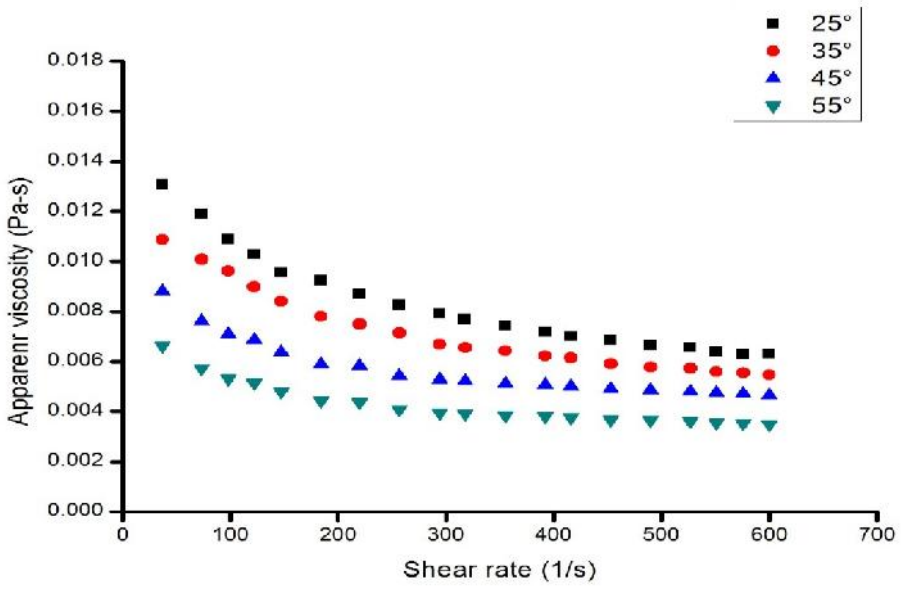

Figure 4.7(b): Variation of apparent viscosity with shear rate of sample S-II at C_w = 60 %

The relative viscosity of slurry suspension with the variation of the temperature is shown in Figure 4.8(a) at 98 s^{-1}. When slurry suspension temperature increases from 25ºC to 35ºC, relative viscosity get reduced 11.66% with 60% concentration, 13.72% with 50% concentration, 5.41% with 40% concentration and 15.34% with 30% concentration respectively. With the increase of slurry temperature from 35ºC to 45ºC, the relative viscosity decrease 26.29%, 23.45%, 30.86% and 28.65% with the 60, 50, 40 and 30% concentration by weight respectively. With the increase of slurry temperature from 45ºC to 55ºC, the relative viscosity decrease 4.23%, 7.39%, 12.63% and 15.22% with the 60, 50, 40 and 30% concentration by weight respectively.

When slurry suspension temperature increases from 25ºC to 35ºC, relative viscosity get reduced 12.65% with 60% concentration, 14.72% with 50% concentration, 15.10% with 40% concentration and 26.8% with 30% concentration respectively. With the increase of slurry temperature from 35ºC to 45ºC, the relative viscosity decrease 16.23%, 21.43%, 21.70% and 26.89% with the 60, 50, 40 and 30% concentration by weight respectively. With the increase of slurry temperature from 45ºC to 55ºC, the relative viscosity decrease 10.41%, 9.37%, 15.90% and 20.22% with the 60, 50, 40 and 30% concentration by weight respectively. Based on the relative viscosity data results in Figure 4.8, the optimum modification temperature found as 45ºC. The relative viscosity reduction was marginal with increasing the temperature from 45ºC to 55°C for all the test shear rate condition.

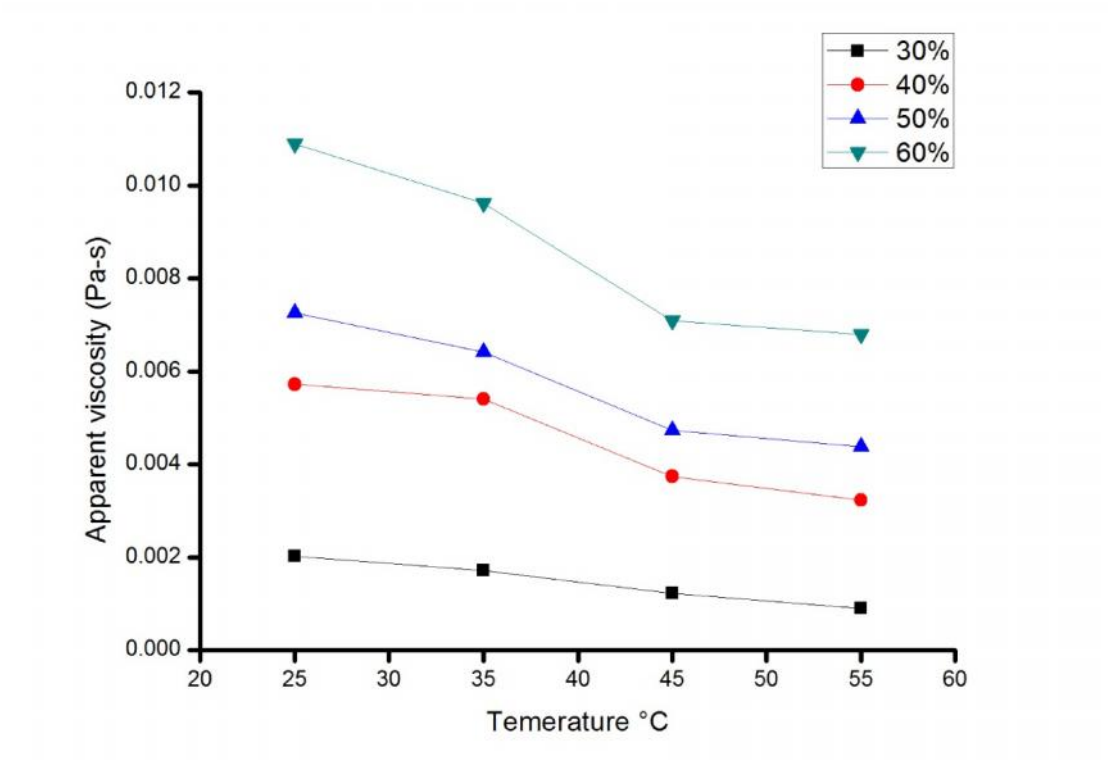

Figure 4.8(a): Variation of apparent viscosity with temperature of sample S-II (98 s^{-1})

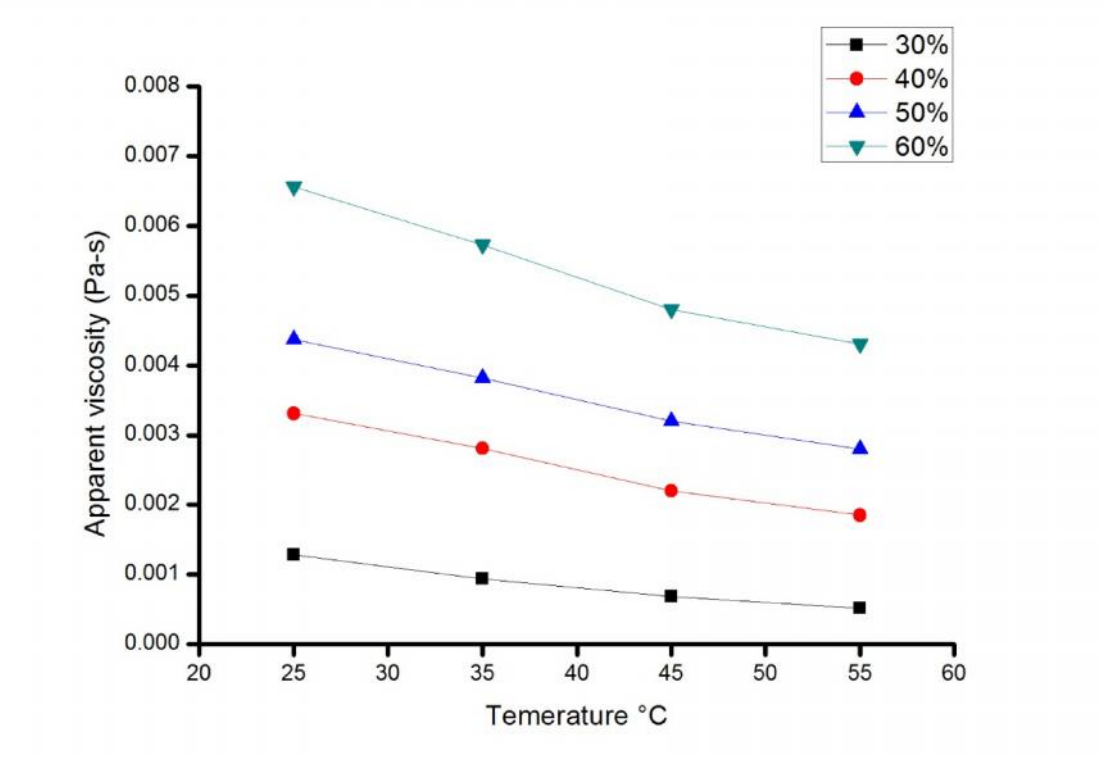

Figure 4.8(b): Variation of apparent viscosity with temperature of sample S-II (527 s^{-1})

CHAPTER 5

INFLUENCE OF PARTICLE GRADATION ON MINERAL SLURRY

5.1 RHEOLOGY EXPERIMENT

The present study considers two different cases for the study of rheological behavior of mineral slurry. The first case considers the unimodal particle size distribution which considers the size of the particle between 53-75 μm and the second case considers the bimodal particle size distribution which considers the certain percentage of particle of size between 53-75 μm and certain percentage of particle between 106-150 μm or 150-250 μm. The temperature of the fluid is maintained constant to 25°C during the experiment using a thermostatically controlled water bath which is connected to viscometer.

5.2 RESULTS AND DISCUSSION

5.2.1 Effect of concentration on rheology of Iron ore slurry

The rheological experiments were conducted with solid weight concentration of 30, 40, 50 and 60% by weight and the shear rate was applied from 0-600 s^{-1} for time interval of 2 minutes to measure the apparent viscosity and shear stress at a given shear rate. The flow curves obtained by the rheological experimentation revealed that the rheological behavior of mineral slurry is immensely affected by the variation in concentration of solids in the slurry. Figure 5.1 shows the variation of shear stress with shear strain for different concentration of coal slurry and Figure 5.2 shows the variation of apparent viscosity with shear rate. From Figure 5.1 and 5.2, it was found that the solids concentration had a considerable effect on rheological behavior of mineral mixture. As solid concentration was increased, the apparent viscosity of mineral mixture increased. The increase in the apparent viscosity with concentration may be due to increase in particle to particle shear interactions increase the resistance. The frictional force between the particles becoming significant and the accompanying resistance is reflected in the increase in viscosity. The shear stress value of the sample slurry increases from 11.78 Pa, 23.17 Pa, 35.03 Pa and 52.55 Pa with the concentration of 30, 40, 50 and 60% by weight respectively at the temperature of 25°C.

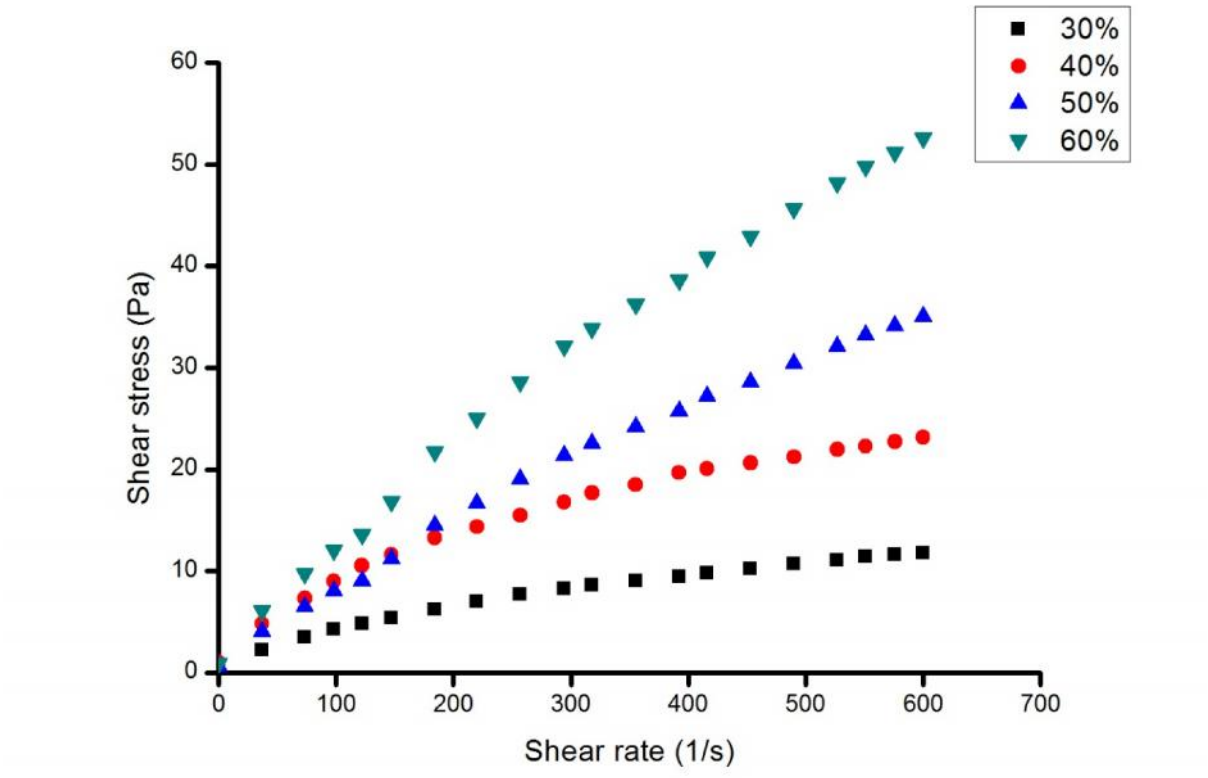

Figure 5.1: Rheogram of iron ore slurry at different concentrations (25°C)

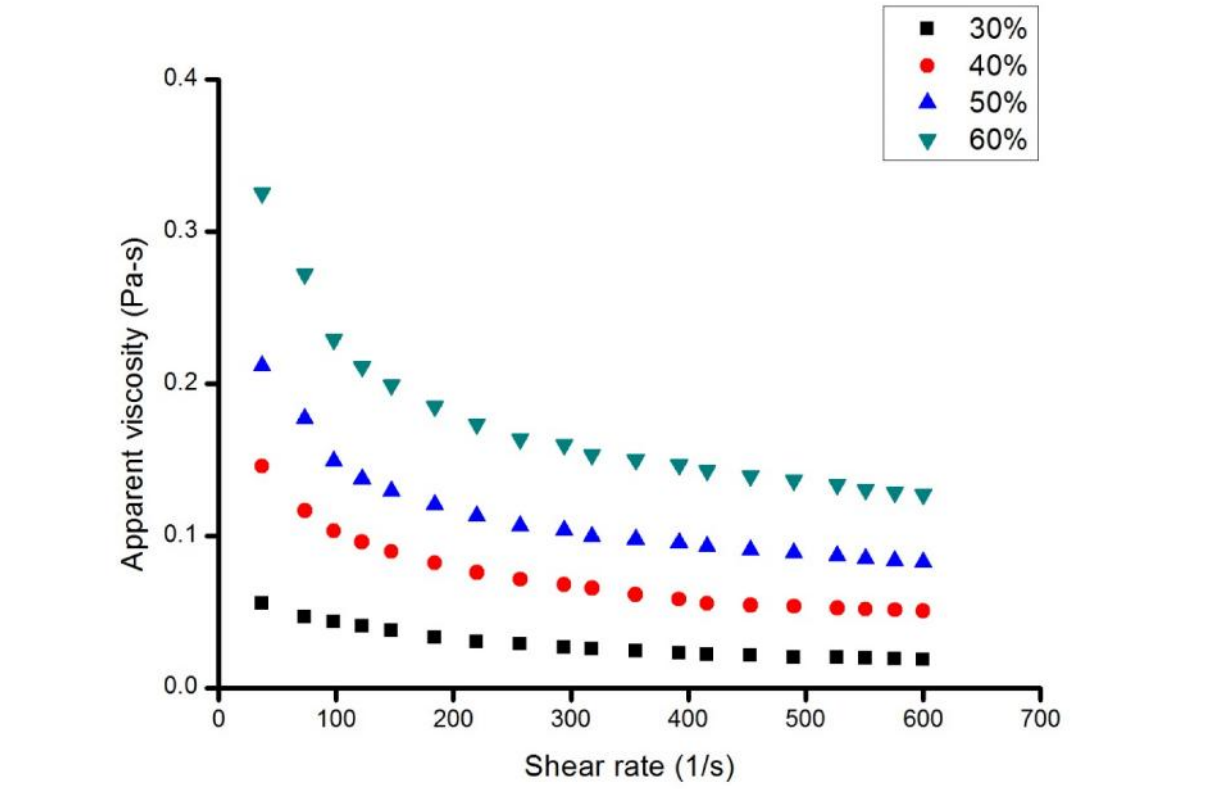

Figure 5.2: Variation of apparent viscosity with shear rate for different concentration of mineral slurry (25°C)

5.2.2 Effect of bimodal particle size distribution on rheology of iron ore slurry

Since the objective of slurry transportation is also to transport the maximum concentration of solid with low viscosity, it is required to find out the optimum concentration of mineral slurry which can be transported with low cost. So the experiment is conducted to determine the rheological behavior of slurry by blending the mineral sample with mixture of coarse and fine particles and hence making a bimodal particle size distribution. The bimodal slurry sample is prepared by mixing the coal particle of size 53- 75 μm with 106-150 μm as well as the coal particle of size 53-75 μm with 150-250 μm with various proportions and the experiment is conducted to study the rheological behavior of coal slurry having over all concentration ranging from 30% to 60%.

Figure 5.3(a-d) shows the variation of apparent viscosity with different shear rate for bimodal slurry having particle size 53-75 μm and 106-150 μm for various concentrations ranging from 30% to 60%. Similarly Fig. 5.4(a-d) shows the variation of apparent viscosity with different shear rate for bimodal slurry having particle size 53-75 μm and 150-250 μm for various concentrations ranging from 30% to 60%. In both the cases, it is found that the apparent viscosity of the slurry is decreased with increase in percentage of coarse particle up to a certain fraction and then increases with increase in percentage of coarse particles. The optimum fraction obtained from both the cases for various concentrations is 20% up to which the apparent viscosity decreases. This indicates the bimodal slurry sample having 20% coarse particle is preferable for transportation in a pipe line.

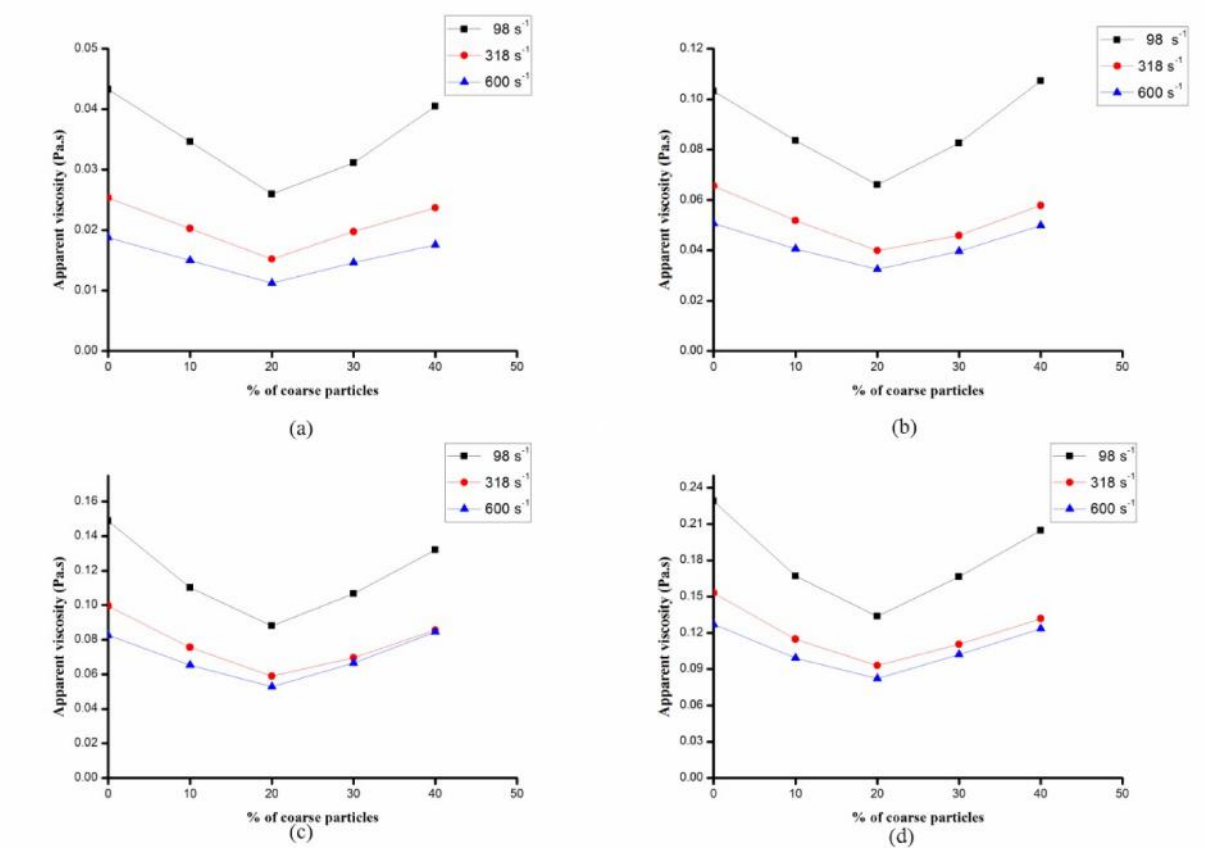

Figure 5.3: Effect of bimodal particle size distribution of size 53-75 µm and 106-150 µm on apparent viscosity of iron ore slurry having a) 30 % Concentration b) 40 % concentration c) 50 % Concentration d) 60 % concentration.

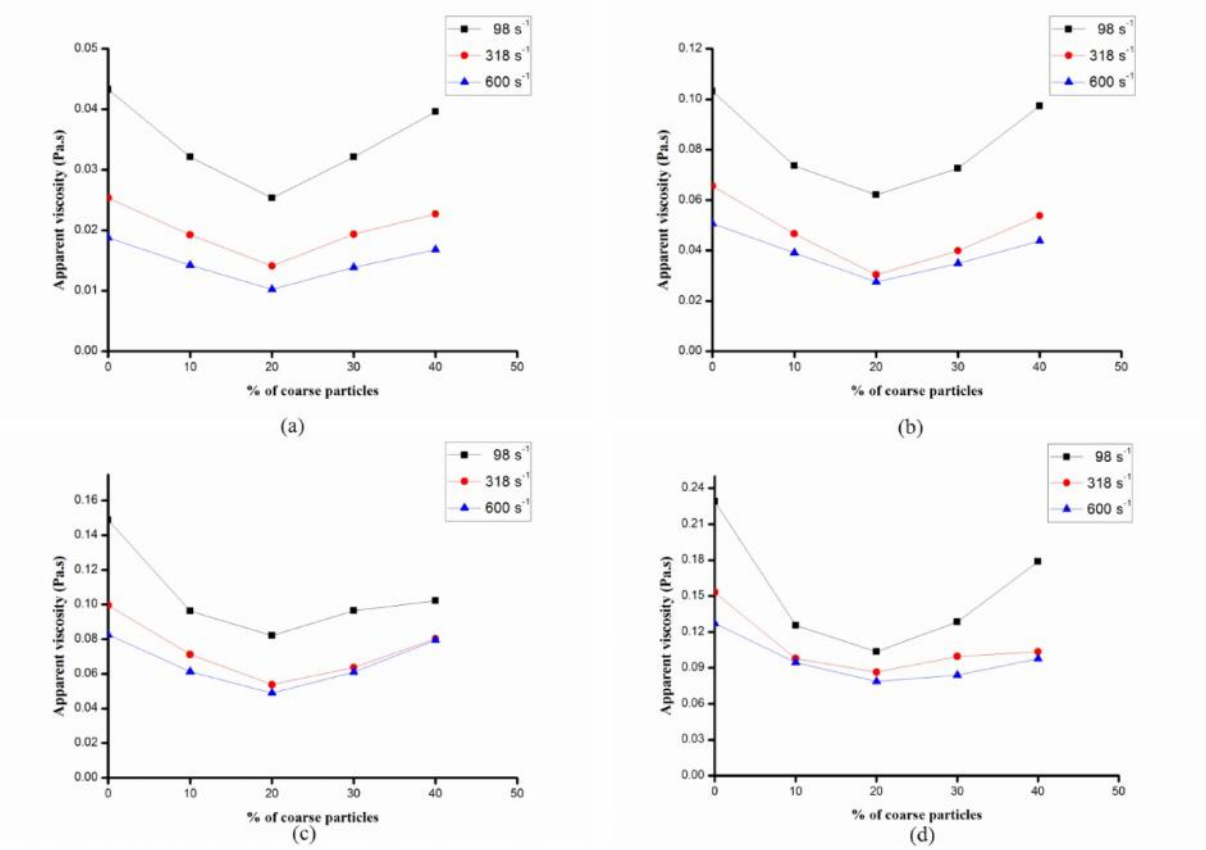

Figure 5.4: Effect of bimodal particle size distribution of size 53-75 µm and 150-250 µm on apparent viscosity of iron ore slurry having a) 30 % Concentration b) 40 % concentration c) 50 % Concentration d) 60 % concentration.

5.2.3 Effect of concentration on rheology of zinc ore slurry

From Figure 5.5 and 5.6, it was found that the solids concentration had a considerable effect on rheological behavior of mineral mixture. As solid concentration was increased, the apparent viscosity of mineral mixture increased. The increase in the apparent viscosity with concentration may be due to increase in particle to particle shear interactions increase the resistance. The frictional force between the particles becoming significant and the accompanying resistance is reflected in the increase in viscosity. The shear stress value of the sample slurry increases from 1.05 Pa, 2.68 Pa, 3.45 Pa and 5.51 Pa with the concentration of 30, 40, 50 and 60% by weight respectively at the temperature of 25°C.

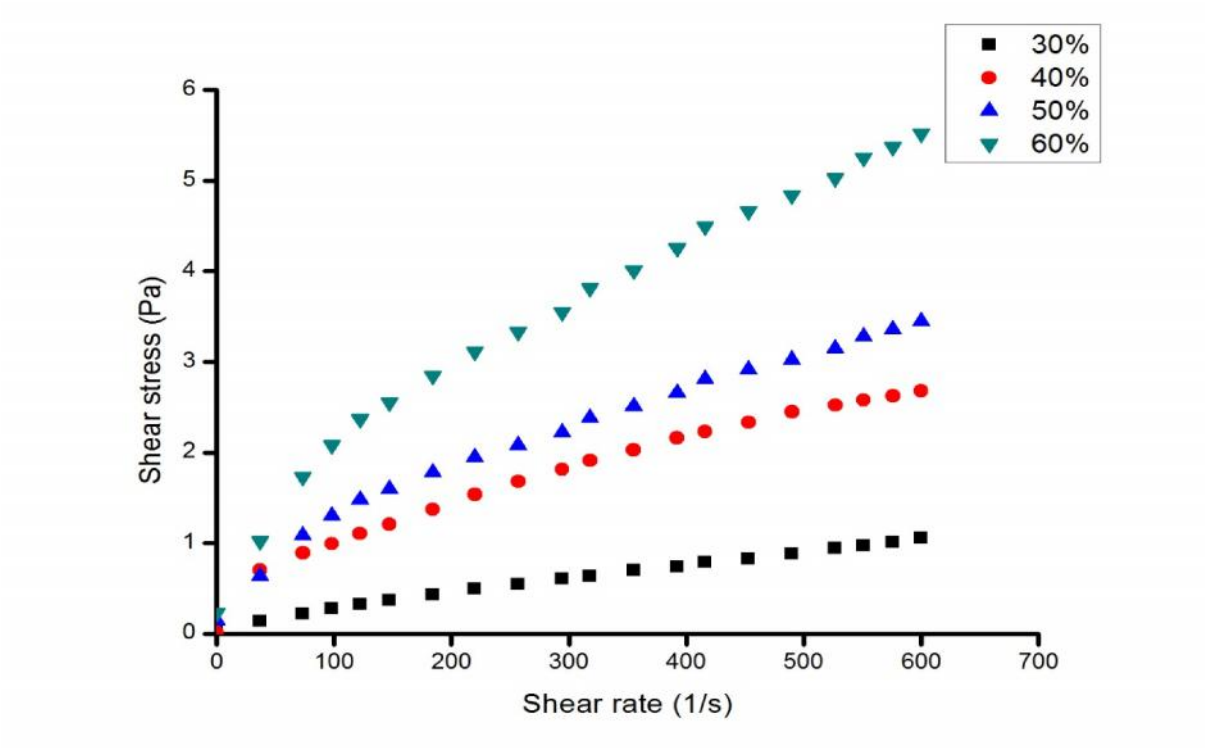

Figure 5.5: Rheogram of zinc ore slurry at different concentrations (25°C)

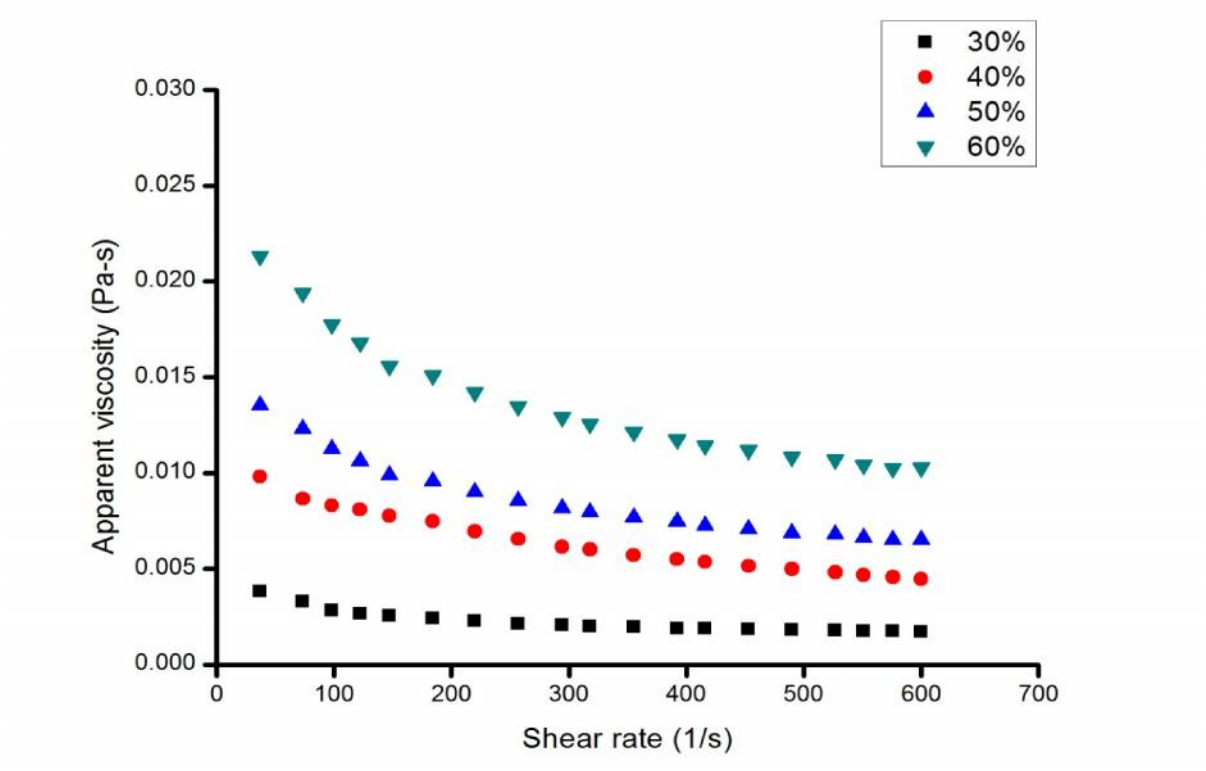

Figure 5.6: Variation of apparent viscosity with shear rate for different concentration of mineral slurry (25°C)

5.2.4 Effect of bimodal particle size distribution on rheology of zinc ore slurry

Figure 5.7(a-d) shows the variation of apparent viscosity with different shear rate for bimodal slurry having particle size 53-75 µm and 106-150 µm for various concentrations ranging from 30% to 60%. Similarly Fig. 5.8(a-d) shows the variation of apparent viscosity with different shear rate for bimodal slurry having particle size 53-75 µm and 150-250 µm for various concentrations ranging from 30% to 60%. In both the cases, it is found that the apparent viscosity of the slurry is decreased with increase in percentage of coarse particle up to a certain fraction and then increases with increase in percentage of coarse particles. The optimum fraction obtained from both the cases for various concentrations is 20% up to which the apparent viscosity decreases. This indicates the bimodal slurry sample having 20% coarse particle is preferable for transportation in a pipe line.

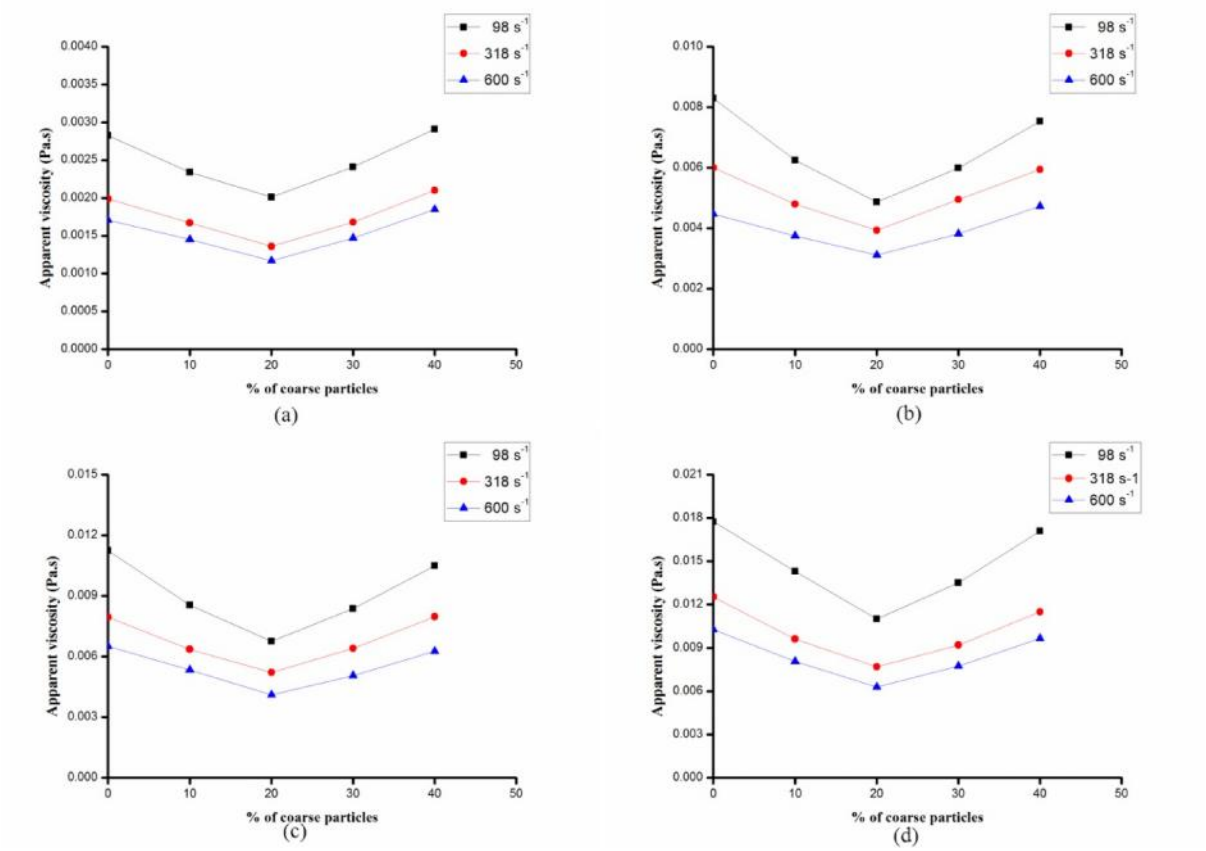

Figure 5.7: Effect of bimodal particle size distribution of size 53-75 µm and 106-150 µm on apparent viscosity of zinc ore slurry having a) 30 % Concentration b) 40 % concentration c) 50 % Concentration d) 60 % concentration.

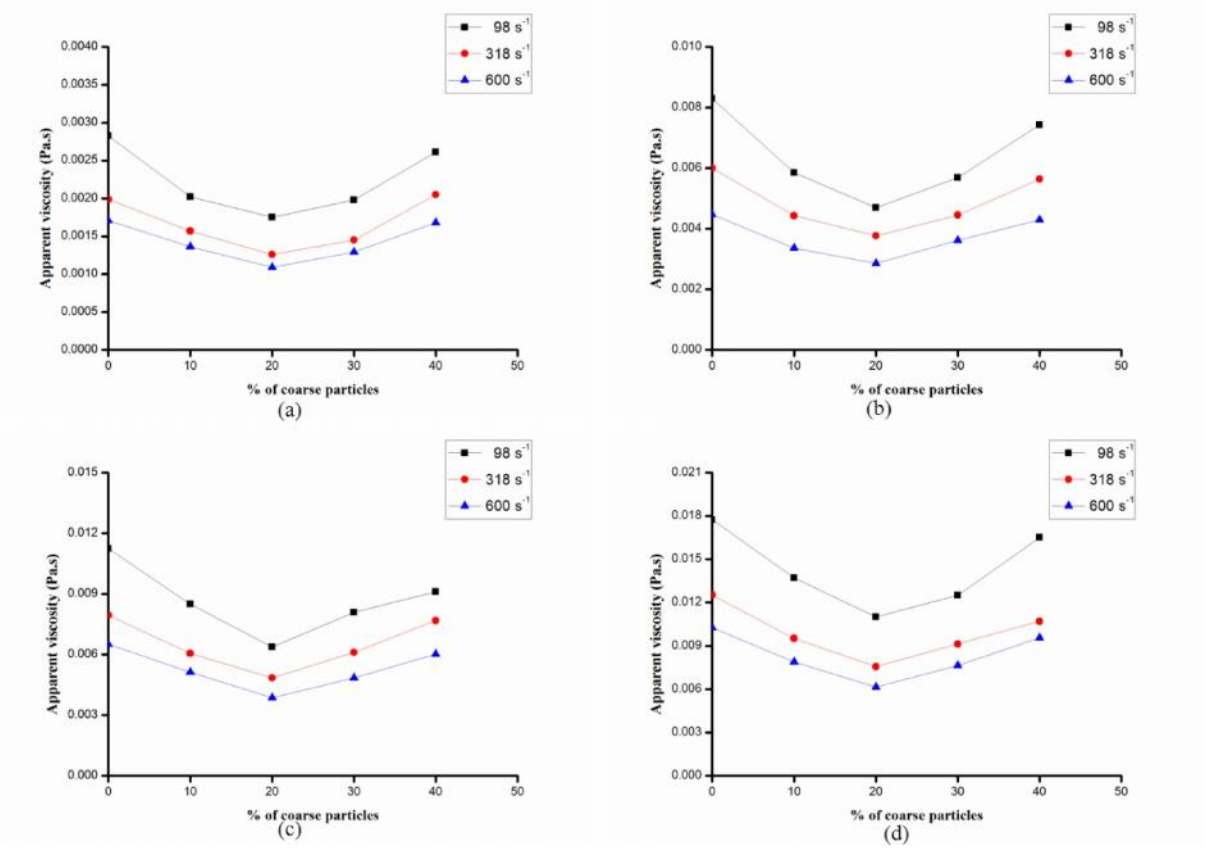

Figure 5.8: Effect of bimodal particle size distribution of size 53-75 µm and 150-250 µm on apparent viscosity of zinc ore slurry having a) 30 % Concentration b) 40 % concentration c) 50 % Concentration d) 60 % concentration.

5.3 HEAD LOSS CALCULATION

Head loss calculation of iron ore slurry at fine particles and mixing of coarser particles at concentration 30-60% by weight was carried out by applying a non-Newtonian head loss model. The particle densities of iron ore at different concentration s were calculated using the following equation:

$$\rho_m = 100 / [c_w / \rho_s + [100 - c_w] / \rho_l] \quad (5.1)$$

Using the power law parameters such as the consistency parameter (K) and flow behavior index (n) obtained from the rheological data, the power law Reynolds number of slurry R_{ep} for a given pipe size and flow velocity was calculated using the following expression

$$R_{ep} = \frac{8D^n V^{2-n} \rho_m}{K} \left\{ \frac{n}{2+6n} \right\}^n \quad (5.2)$$

Flow is considered as laminar and the laminar flow friction factor (f) can be determined from the equation

$$f = \frac{16}{R_{ep}} \quad (5.3)$$

In the present analysis, the computation of head loss for iron ore fine particles and mixture coarser particles was carried out in the slurry velocity range of 0.5 to 2 m/s, since the effect of pipe roughness is negligible under laminar pipe flow situations. The head loss gradient of slurry in meter of water per meter length of pipe, h was then computed by using the Fanning's equation given as

$$h = \frac{2fV^2}{gD} \frac{\rho_m}{\rho_w} \quad (5.4)$$

The head loss of iron ore fine particle and with coarser particles were calculated at weight concentrations of 30, 40, 50 and 60% for pipe size having diameter 100mm. The velocity versus head loss of iron ore slurry at different weight concentrations in a 100

mm diameter pipeline is shown in Figure 5.9. As expected the head loss values increased with increase in weight concentration.

Table 5.1: Variation of power law parameters, n and K with solids concentration and Coarser fractions of iron ore slurry.

Coarser Fraction	30%		40%		50%		60%	
	n	k	n	k	n	k	n	k
0	0.479	0.521	0.468	3.658	0.455	5.453	0.448	7.421
0.1	0.481	0.504	0.471	3.476	0.458	5.357	0.452	7.247
0.2	0.484	0.489	0.473	3.296	0.463	5.184	0.455	7.024
0.3	0.489	0.462	0.475	2.967	0.467	4.972	0.459	6.957
0.4	0.494	0.437	0.479	2.765	0.472	4.846	0.462	6.749

Table 5.2: Variation of power law parameters, n and K with solids concentration and Coarser fractions of zinc ore slurry.

Coarser Fraction	30%		40%		50%		60%	
	n	k	n	k	n	k	n	k
0	0.626	0.0172	0.601	0.0723	0.586	0.267	0.564	0.486
0.1	0.638	0.0165	0.606	0.0702	0.59	0.255	0.569	0.474
0.2	0.642	0.0157	0.612	0.0687	0.595	0.241	0.572	0.443
0.3	0.648	0.0149	0.618	0.0675	0.6	0.228	0.577	0.421
0.4	0.654	0.0141	0.625	0.0662	0.603	0.211	0.581	0.402

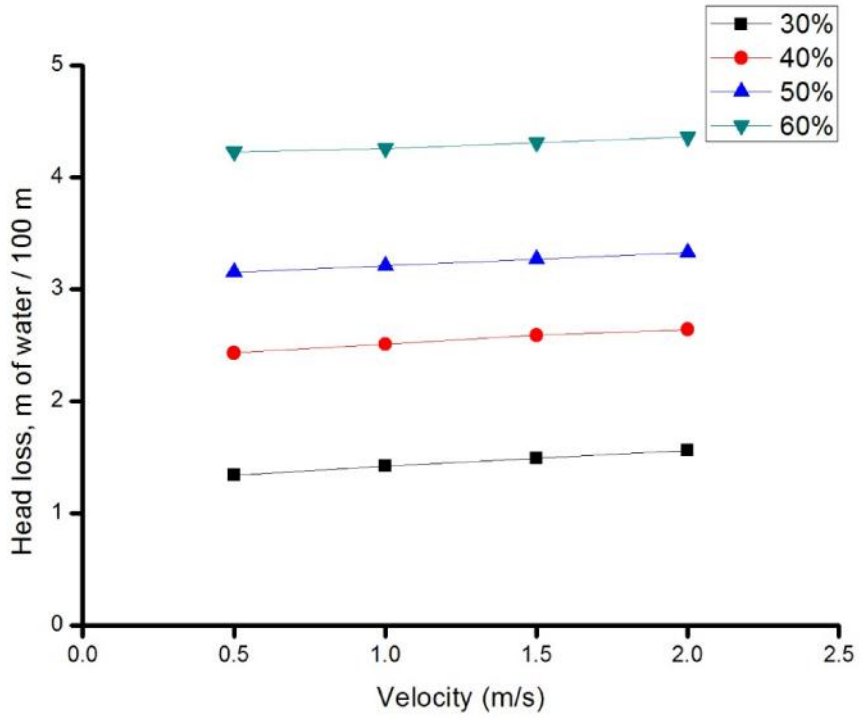

Figure 5.9: Head loss of fly ash slurry at different weight concentration of iron ore slurry, pipe diameter=100mm.

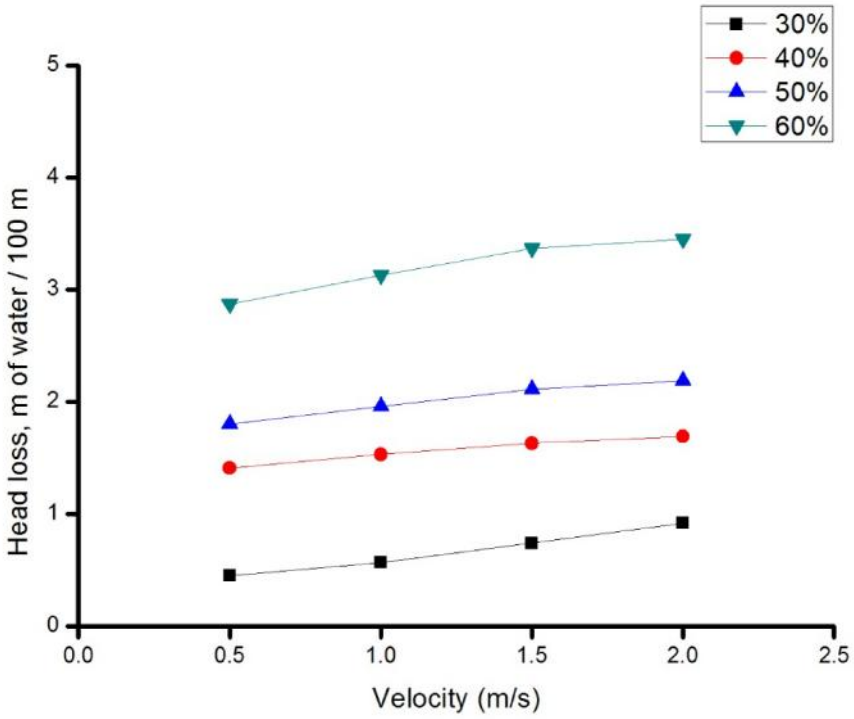

Figure 5.10: Head loss of fly ash slurry at different weight concentration of zinc ore slurry of, pipe diameter=100mm.

5.3.1 Effect of addition of coarser fractions on head loss of mixture slurry

Figure 5.11 and 5.12 shows the effect of addition of coarser fractions on the slurry head loss at different pipe flow velocities for a 100 mm diameter pipeline. It is observed from the figure that the head loss value decreased with the addition of coarser fractions at a specific overall weight concentration of the slurry. The reasons, for this reduction in head loss, may be attributed to the particle–particle and particle–fluid friction that occurs during slurry flow. Addition of coarse fractions with relatively higher particle sizes reduces the effective surface area of the particles thereby, reducing the degree of friction in the slurry. It is also observed that the, reduction in pressure drop of iron ore slurry at high solid concentrations is more as compared to low solid concentrations with mixing coarser particles. The maximum reduction in pressure drop marked as 8.20, 9.15, 11.40 and 12.17% at 30% (by weight) and 4.72, 6.33, 6.49 and 8.25% at 60% (by weight) for the iron ore slurry as shown in figure 5.11 whereas The maximum reduction in pressure drop marked as 14.55, 25.45, 17.40 and 18.17% at 30% (by weight) and 4.52, 6.38, 7.49 and 10.25% at 60% (by weight) for the zinc ore slurry as shown in figure 5.12.

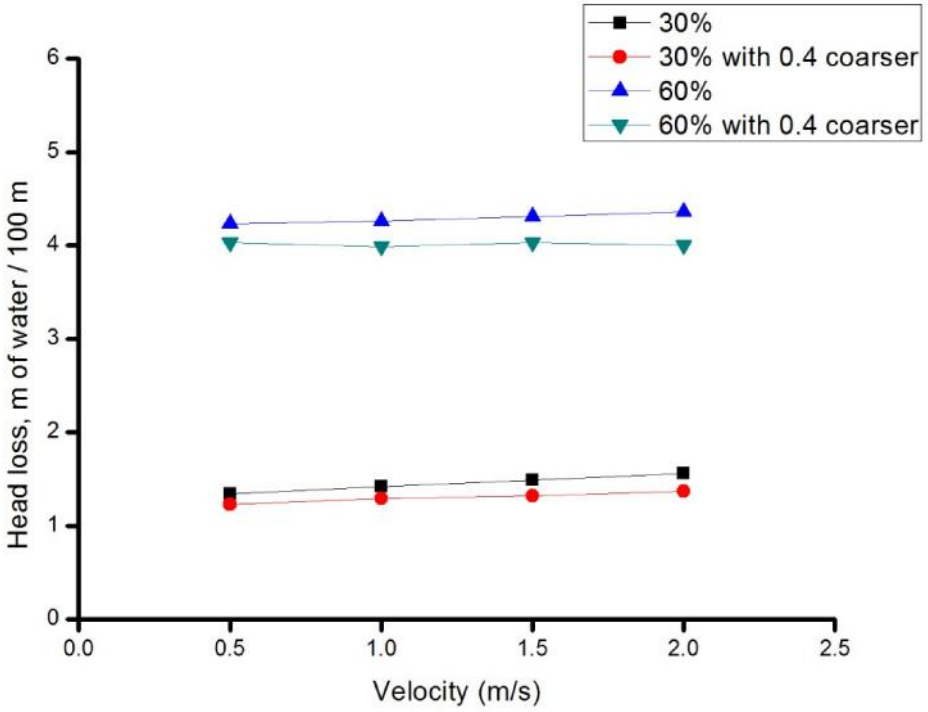

Figure 5.11: Effect of addition of coarser fraction on head loss of at different concentrations of iron ore slurry, pipe diameter=100 mm.

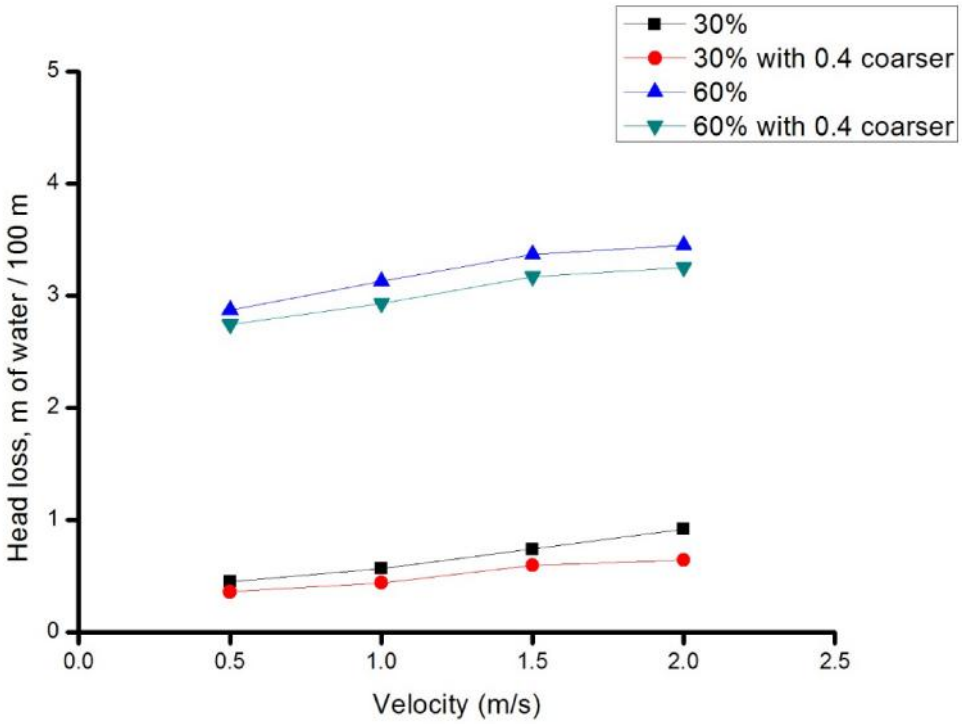

Figure 5.12: Effect of addition of coarser fraction on head loss of at different concentrations of zinc ore slurry, pipe diameter=100 mm.

CHAPTER 6

CONCLUSIONS AND FUTURE SCOPE

6.1 CONCLUSIONS

The present research work was carried out on four mineral sample viz. iron ore (hematite), zinc ore, iron ore (magnetite) and lime. The comprehensive characterization was carried out to determine the various properties like mineral content, particle size distribution, morphology and pH value of mineral samples. The detailed flow characteristics of iron ore and zinc slurry suspension was analysed and conclusions are as under:

- The slurry suspension shows Newtonian behaviour upto 30% solid concentration and beyond behave as non-Newtonian in nature.
- With increase in the concentration, both apparent viscosity and shear stress increases whereas with the increase in temperature, both apparent viscosity and shear stress decreases.
- The rheological behaviour of finer particulate mineral suspension has improved with the addition of the coarse particulate
- The optimum value of viscosity found with 20% addition of coarser particles in the finer particles.
- The addition of coarser particle in the sample slurry reduces the pressure drop and can result in substantial saving in energy consumption.

6.2 FUTURE SCOPE

The present aim of the study is to find the rheological behaviour and generated data is used for calculating the pressure drop in the slurry pipeline by using Fanning's equation. The various works that can extend the present study are:

- Investigation of rheological behaviour in the presence of additives.
- Investigation of rheological slurry by using graph theory.
- Investigation of rheological slurry by computational fluid dynamics.

REFERENCES

1. Yavuz R. and Kucukbayrak S. (1998): "Effect of particle size distribution on Rheology of Lignite-Water Slurry", *Energy sources*, 20(9):787-794.
2. Mishra S.K., Senapati P.K. and Panda D. (2002): "Rheological behavior of Coal Water Slurry", *Energy Sources, Part A: Recovery, Utilization, and Environmental Effects*, 24:159-167.
3. Lei Li, Usui Hiromoto and Suzuki Hiroshi (2002): "Study of pipeline transportation of dense fly ash-water slurry", *Coal preparation*, 22(2):65-80.
4. Hiroya A., Naitoa Makio, Hottab Tadashi, Kamiyac Hidehiro and Uematsu Keizo (2003): "Pore defects related to slurry character and their relevance to strength distribution in alumina ceramics", *Powder Technology*, 134:58– 64.
5. Dincer H., Boylu F., Sirkeci A.A. and Atesok G. (2003): "The effect of chemicals on the viscosity and stability of coal water slurries", *International Journal of Mineral Processing*, 70:41-51.
6. Boylu F., Dincer H. and Atesok G. (2004): "Effect of coal particle size distribution, volume fraction and rank on the rheology of coal water slurries", *Fuel Processing Technology*, 85:241– 250.
7. Park C.K., Noh M.H. and Park T.H. (2005): "Rheological properties of cementitious materials containing mineral admixtures", *Cement and Concrete Research*, 35:842– 849.
8. Ferraris Chiara F., Karthik H. Obla and Russell Hill (2005): "The influence of mineral admixtures on the rheology of cement paste and concrete", *Cement and Concrete Research*, 31:245-255.
9. Yuchi W., Li B., Li W. and Chen H. (2005): "Effects of coal characteristics on the properties of coal water slurry", *Coal Preparation*, 25:239-249.
10. Senapati P.K., Das D., Nayak A. and Mishra P.K. (2008): "Studies on preparation of coal water slurry using a natural additive", *Energy Sources, Part A: Recovery, Utilization, and Environmental Effects*, 30:1788-1796.
11. Shukla S.C., Kukade S., Mandal S.K. and Kundu G. (2008): "Coal–oil–water multiphase fuel: Rheological behavior and prediction of optimum particle size", *Fuel*, 87:3428–3432.

12. Mosa Eisa S., Abdel-Hady M. Saleh, Taha A., Anas M. El-Molla (2008): "Effect of chemical additives on flow characteristics of coal slurries", *Physicochemical Problems of Mineral Processing*, 42:107-118.
13. Das D., Panigrahi S., Misra P.K. and Nayak A. (2008): "Effect of organized assemblies, Formulation of highly concentrated coal-water slurry using a natural surfactant", *Energy & Fuels*, 22:1865–1872.
14. Zhou M., Pan B., Yang D., Lou H. and Qiu X. (2010): "Rheological behaviour investigation of concentrated coal-water suspension", *Journal of Dispersion Science and Technology*, 31:838-843.
15. Ruiz-Agudo E. and Rodriguez-Navarro C. (2010): "Microstructure and Rheology of Lime Putty", *Langmuir*, 26(6):3868–3877.
16. Bentz Dale P., Chiara F. Ferraris and Michael A. Galler (2012): "Influence of Particle Size Distributions on Yield Stress and Viscosity of Cement-Fly Ash Pastes", *Cement and Concrete Research*, 42 (2):404-409.
17. Buranasrisak P. and Narasingha M.H. (2012): "Effects of particle size distribution and packing characteristics on the preparation of highly-loaded coal-water slurry", *International Journal of Chemical Engineering and Application*, 3:31-35.
18. Marcos Gomes Vieira and Antonio Eduardo Clark Peres (2013): "Effect of rheology and dispersion degree on the regrinding of an iron ore concentrate", *masterres technology*,2(4):332–339.
19. Toru Shimizu, Matsuura Kazuhiro, Furue Harumi and Matsuzak Kunio (2013): "Thermal conductivity of high porosity alumina refractory bricks made by a slurry gelation and foaming method", *Journal of the European Ceramic Society*, 33:3429– 3435.
20. Kirk Vance, Kumar Aditya, Sant Gaurav and Neithalath Narayanan (2013): "The rheological properties of ternary binders containing Portland cement, limestone, and metakaolin or fly ash", *Cement and Concrete Research*, 52:196–207.
21. Chen J.J., Kwan A.K.H. and Jiang Y. (2014): "Adding limestone fines as cement paste replacement to reduce water permeability and sorptivity of concrete", *Construction and Building Materials*, 56:87–93.

22. Seddik Meddah Mohammed, Lmbachiya Mukesh C. and Dhir Ravindra K. (2014): “Potential use of binary and composite limestone cements in concrete production”, *Construction and Building Materials*, 58:193–205.
23. Singh Mani, Ratha Dwarikanath, Kumar Satish and Kumar Deepak (2015): “Influence of particle size distribution and temperature on rheological behaviour of coal slurry”, *DOI*: 10.1080/19392699.2015.1049265.

APPENDIX

Table A1: Rheology of iron ore slurry at c_w = 30 % by weight at 25°C

Shear rate (1/s)	Shear stress (Pa)	Apparent viscosity (Pa-s)
0	0.425	
36.8	1.46	0.0397
73.5	2.26	0.0334
98	2.76	0.0309
122	3.16	0.0289
147	3.53	0.0269
184	4.05	0.0235
220	4.57	0.0217
257	5.02	0.0206
294	5.39	0.0191
318	5.62	0.0181
355	5.91	0.0173
392	6.18	0.0163
416	6.39	0.0157
453	6.67	0.0151
490	6.99	0.0143
527	7.24	0.0141
551	7.47	0.0139
576	7.6	0.0137
600	7.7	0.0134

Table A2: Rheology of iron ore slurry at c_w = 30 % by weight at 45°C

Shear rate (1/s)	Shear stress (Pa)	Apparent viscosity (Pa-s)
0	0.23	##
36.8	0.913	0.0248
73.5	1.43	0.0195
98	1.72	0.0183
122	2.02	0.0174
147	2.38	0.0163
184	2.75	0.0151
220	3.12	0.0139
257	3.36	0.0125
294	3.61	0.0113
318	3.76	0.0104
355	3.97	0.00939
392	4.17	0.00846
416	4.32	0.0077
453	4.51	0.00705
490	4.75	0.00691
527	4.93	0.00657
551	5.04	0.00649
576	5.19	0.00641
600	5.31	0.00637

Table A3: Rheology of iron ore slurry at c_u = 50 % by weight at 25°C

Shear rate (1/s)	Shear stress (Pa)	Apparent viscosity (Pa-s)
0	0.4	##
36.8	2.66	0.134
73.5	4.23	0.112
98	5.24	0.0942
122	5.91	0.0869
147	7.33	0.082
184	9.46	0.0762
220	10.89	0.0714
257	12.45	0.0673
294	13.99	0.0657
318	14.76	0.063
355	15.8	0.0618
392	16.83	0.0603
416	17.8	0.0589
453	18.7	0.0572
490	19.9	0.0561
527	21	0.0549
551	21.7	0.0536
576	22.3	0.0529
600	22.9	0.0523

Table A4: Rheology of iron ore slurry at c_u = 50 % by weight at 45°C

Shear rate (1/s)	Shear stress (Pa)	Apparent viscosity (Pa-s)
0	0.2	##
36.8	1.39	0.0958
73.5	2.08	0.0783
98	2.83	0.0729
122	3.59	0.0663
147	4.45	0.0603
184	5.73	0.0532
220	7.25	0.0478
257	8.72	0.0439
294	10.02	0.0396
318	10.8	0.036
355	12.1	0.034
392	13	0.0333
416	13.9	0.0329
453	15	0.0325
490	16.2	0.032
527	17.4	0.0316
551	18.1	0.0311
576	18.9	0.0307
600	19.7	0.0301

Table B1: Rheology of zinc ore slurry at c_u = 30 % by weight at 25°C

Shear rate (1/s)	Shear stress (Pa)	Apparent viscosity (Pa-s)
0	0.015	##
36.8	0.099	0.00272
73.5	0.157	0.00234
98	0.198	0.00202
122	0.232	0.0019
147	0.264	0.00183
184	0.31	0.00171
220	0.356	0.00161
257	0.387	0.00151
294	0.432	0.00147
318	0.453	0.00142
355	0.498	0.0014
392	0.529	0.00135
416	0.563	0.00135
453	0.592	0.00131
490	0.631	0.00129
527	0.675	0.00128
551	0.695	0.00125
576	0.719	0.00124
600	0.753	0.00122

Table B2: Rheology of iron ore slurry at c_u = 30 % by weight at 45°C

Shear rate (1/s)	Shear stress (Pa)	Apparent viscosity (Pa-s)
0	0.012	##
36.8	0.0597	0.00162
73.5	0.0989	0.00137
98	0.134	0.00122
122	0.161	0.00115
147	0.192	0.00111
184	0.226	0.00103
220	0.253	9.85E-04
257	0.277	9.58E-04
294	0.307	9.11E-04
318	0.322	8.92E-04
355	0.356	8.53E-04
392	0.389	8.13E-04
416	0.413	7.85E-04
453	0.443	7.37E-04
490	0.472	7.15E-04
527	0.504	6.85E-04
551	0.522	6.48E-04
576	0.544	6.19E-04
600	0.56	5.99E-04

Table B3: Rheology of zinc ore slurry at c_w = 50 % by weight at 25°C

Shear rate (1/s)	Shear stress (Pa)	Apparent viscosity (Pa-s)
0	0.0956	##
36.8	0.42	0.00872
73.5	0.713	0.00793
98	0.856	0.00726
122	0.974	0.00686
147	1.05	0.00637
184	1.17	0.00616
220	1.28	0.0058
257	1.37	0.00551
294	1.46	0.00527
318	1.57	0.00513
355	1.65	0.00495
392	1.75	0.0048
416	1.85	0.00467
453	1.92	0.00457
490	1.99	0.00443
527	2.07	0.00437
551	2.16	0.00426
576	2.21	0.00419
600	2.27	0.0042

Table B4: Rheology of zinc ore slurry at c_w = 50 % by weight at 45°C

Shear rate (1/s)	Shear stress (Pa)	Apparent viscosity (Pa-s)
0	0.0656	##
36.8	0.35	0.00588
73.5	0.524	0.00508
98	0.662	0.00473
122	0.775	0.00457
147	0.814	0.00425
184	0.883	0.00393
220	0.966	0.00388
257	1.06	0.00361
294	1.17	0.00351
318	1.23	0.00348
355	1.34	0.00341
392	1.4	0.00337
416	1.46	0.00334
453	1.53	0.00327
490	1.61	0.00324
527	1.7	0.0032
551	1.76	0.00316
576	1.81	0.00313
600	1.87	0.0031

Table C1: Variation of Pressure drop at different concentration of iron ore slurry

Velocity	Concentration (by weight)			
	30%	40%	50%	60%
0.5	1.34	2.43	3.15	4.23
1	1.42	2.51	3.21	4.26
1.5	1.49	2.59	3.27	4.31
2	1.56	2.64	3.33	4.36

Table C2: Variation of Pressure drop of iron ore slurry when mixing with 0.4 coarser particle

Velocity	Concentration (by weight)			
	30%	30% with 0.4 coarser particle	60%	60% with 0.4 coarser particle
0.5	1.34	1.23	4.23	4.03
1	1.42	1.29	4.26	3.99
1.5	1.49	1.32	4.31	4.03
2	1.56	1.37	4.36	4

Table D1: Variation of Pressure drop at different concentration of zinc ore slurry

Velocity	Concentration (by weight)			
	30%	40%	50%	60%
0.5	0.45	1.41	1.8	2.87
1	0.57	1.53	1.96	3.13
1.5	0.74	1.63	2.11	3.37
2	0.92	1.69	2.19	3.45

Table D2: Variation of Pressure drop of zinc ore slurry when mixing with 0.4 coarser particle

Velocity	Concentration (by weight)			
	30%	30% with 0.4 coarser particle	60%	60% with 0.4 coarser particle
0.5	0.45	0.242	2.87	2.55
1	0.57	0.342	3.13	2.84
1.5	0.74	0.497	3.37	2.96
2	0.92	0.544	3.45	3.06